AD-A169 275 CAVITATION SUSCEPTIBILITY MEASUREMENTS OF OCEAN LAKE AND LABORATORY WATERS(U) DAVID W TAYLOR NAVAL SHIP RESEARCH AND DEVELOPMENT CENTER BETHESDA MD Y T SHEN ET AL. MAY 86 DTNSRDC-86/019 F/G 20/4 1/1

UNCLASSIFIED NL

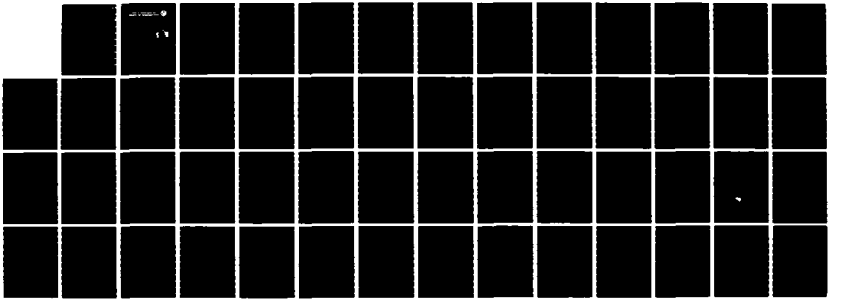

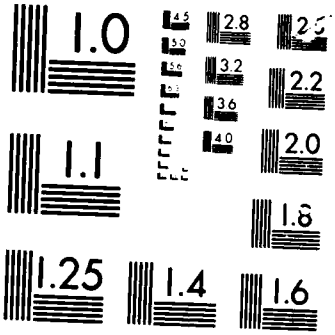

# DAVID W. TAYLOR NAVAL SHIP RESEARCH AND DEVELOPMENT CENTER

Bethesda, Maryland 20084-5000

## CAVITATION SUSCEPTIBILITY MEASUREMENTS OF OCEAN, LAKE AND LABORATORY WATERS

by

Young T. Shen
Scott Gowing
Bruce Edelstein



APPROVED FOR PUBLIC RELEASE; DISTRIBUTION IS UNLIMITED.



SHIP PERFORMANCE DEPARTMENT
RESEARCH AND DEVELOPMENT REPORT

May 1986

DTNSRDC-86/019

CAVITATION SUSCEPTIBILITY MEASUREMENTS OF OCEAN LAKE AND LABORATORY WATERS

UNCLASSIFIED
SECURITY CLASSIFICATION OF THIS PAGE

# REPORT DOCUMENTATION PAGE

| | |
|---|---|
| 1a REPORT SECURITY CLASSIFICATION<br>UNCLASSIFIED | 1b RESTRICTIVE MARKINGS<br>AD-A169275 |
| 2a SECURITY CLASSIFICATION AUTHORITY | 3 DISTRIBUTION/AVAILABILITY OF REPORT<br>APPROVED FOR PUBLIC RELEASE; DISTRIBUTION IS UNLIMITED. |
| 2b DECLASSIFICATION/DOWNGRADING SCHEDULE | |
| 4 PERFORMING ORGANIZATION REPORT NUMBER(S)<br>DTNSRDC-86/019 | 5 MONITORING ORGANIZATION REPORT NUMBER(S) |
| 6a NAME OF PERFORMING ORGANIZATION<br>David W. Taylor Naval Ship R&D Center<br>6b OFFICE SYMBOL (If applicable)<br>Code 1542 | 7a NAME OF MONITORING ORGANIZATION |
| 6c ADDRESS (City, State, and ZIP Code)<br>Bethesda, Maryland 20084-5000 | 7b ADDRESS (City, State, and ZIP Code) |
| 8a NAME OF FUNDING/SPONSORING ORGANIZATION<br>Naval Sea Systems Command<br>8b OFFICE SYMBOL (If applicable)<br>05R | 9 PROCUREMENT INSTRUMENT IDENTIFICATION NUMBER |
| 8c ADDRESS (City, State, and ZIP Code)<br>Washington, D.C. 20262 | 10 SOURCE OF FUNDING NUMBERS<br>PROGRAM ELEMENT NO: 62543N; PROJECT NO: SF 43-434; TASK NO:; WORK UNIT ACCESSION NO: DN378001 |

11 TITLE (Include Security Classification)
CAVITATION SUSCEPTIBILITY MEASUREMENTS OF OCEAN, LAKE AND LABORATORY WATERS

12 PERSONAL AUTHOR(S)
Shen, Young T., Gowing, Scott, and Eckstein, Bruce

| 13a TYPE OF REPORT | 13b TIME COVERED | 14 DATE OF REPORT (Year, Month, Day) | 15 PAGE COUNT |
|---|---|---|---|
| Final | FROM _____ TO _____ | 1986, May | 51 |

16 SUPPLEMENTARY NOTATION

| 17 COSATI CODES | | |
|---|---|---|
| FIELD | GROUP | SUB-GROUP |
| | | |
| | | |

18 SUBJECT TERMS (Continue on reverse if necessary and identify by block number)
Cavitation Measurement
Cavitation Susceptibility
Cavitation in Ocean, Lakes, and Laboratory Waters

19 ABSTRACT (Continue on reverse if necessary and identify by block number)

Experiments have been carried out in laboratories to relate cavitation inception and nuclei distributions. The existence of a strong relationship between cavitation and nuclei has been documented for laboratory waters, but little information is available about ocean waters. Towards this end, ocean and lake measurements were carried out in Exuma Sound, the Gulf Stream off the coast of Florida, and Lake Pend Oreille to provide comparative results in different bodies of water. The test program included cavitation susceptibility measurements by a venturi system, nuclei population measurements by a light scattering device, and a series of standard oceanographic measurements. The depths covered ranged from 10 to 200 m, deeper than ever before for these types of measurements. To provide a reference for comparison between laboratory and natural waters, the same measuring devices were used in the DTNSRDC 12-in. variable pressure water tunnel.

(Continued on reverse side)

| 20 DISTRIBUTION/AVAILABILITY OF ABSTRACT | 21 ABSTRACT SECURITY CLASSIFICATION |
|---|---|
| ☐ UNCLASSIFIED/UNLIMITED ☒ SAME AS RPT ☐ DTIC USERS | UNCLASSIFIED |
| 22a NAME OF RESPONSIBLE INDIVIDUAL<br>Young T. Shen | 22b TELEPHONE (Include Area Code)<br>(301) 227-1339<br>22c OFFICE SYMBOL<br>Code 1542 |

DD FORM 1473, 84 MAR 83 APR edition may be used until exhausted
All other editions are obsolete

SECURITY CLASSIFICATION OF THIS PAGE
UNCLASSIFIED

(Block 19 continued)

There was no difficulty inducing cavitation throughout the test matrix. At depths less than 100 m, the water in the Gulf Stream was found to cavitate more easily than the water in Exuma Sound. At deeper depths, the opposite trend was found. Depending on the nuclei populations, variations of the cavitation inception indices with depth took different forms in Exuma Sound, the Gulf Stream, and Lake Pend Oreille waters. Except at the shallow depths, the lake water was found to be less susceptible to cavitation than the ocean waters. Bubble instability theory and the Rayleigh-Plesset dynamic equation provide good explanations of many of the observed phenomena. The postulation of a critical bubble radius is used to explain the unexpected phenomenon that the concentration of unstable bubbles can increase with depth.

TABLE OF CONTENTS



LIST OF FIGURES

## LIST OF FIGURES (Continued)

## LIST OF TABLES

## ABSTRACT

Experiments have been carried out in laboratories to relate cavitation inception and nuclei distributions. The existence of a strong relationship between cavitation and nuclei has been documented for laboratory waters, but little information is available about ocean waters. Towards this end, ocean and lake measurements were carried out in Exuma Sound, the Gulf Stream off the coast of Florida, and Lake Pend Oreille to provide comparative results in different bodies of water. The test program included cavitation susceptibility measurements by a venturi system, nuclei population measurements by a light scattering device, and a series of standard oceanographic measurements. The depths covered ranged from 10 to 200 m, deeper than ever before for these types of measurement. To provide a reference for comparison between laboratory and natural waters, the same measuring devices were used in the DTNSRDC 12-in. variable pressure water tunnel.

There was no difficulty inducing cavitation throughout the test matrix. At depths less than 100 m, the water in the Gulf Stream was found to cavitate more easily than the water in Exuma Sound. At deeper depths, the opposite trend was found. Depending on the nuclei populations, variations of the cavitation inception indices with depth took different forms in Exuma Sound, the Gulf Stream, and Lake Pend Oreille waters. Except at the shallow depths, the lake water was found to be less susceptible to cavitation than the ocean waters. Bubble instability theory and the Rayleigh-Plesset dynamic equation provide good explanations of many of the observed phenomena. The postulation of a critical bubble radius is used to explain the unexpected phenomenon that the concentration of unstable bubbles can increase with depth.



## ADMINISTRATIVE INFORMATION

This project was supported by the Ship and Submarine Technology Program Element 62543N Propulsor Subproject SF 43-434 at NAVSEA.


## INTRODUCTION

Most hydrofoils or propellers will develop tip vortex and surface cavitation at high speeds. The occurrence of cavitation leads to undesirable changes in hydrodynamic performance, noise generation, and physical damage from vibration and erosion. Therefore, the ability to predict the occurrence of cavitation is an important engineering problem. The prediction of cavitation inception performance has relied heavily on model experiments and extrapolation of the model results to full scale because of the complexity of physical processes involved with cavitation inception. Full-scale evaluations are often conducted and correlated with the model data.

Present knowledge is inadequate to always accurately evaluate and predict cavitation performance both in laboratories and in oceans. In laboratories, it has often been observed that cavitation takes a variety of forms which may differ from facility to facility with similar models or even the same model. Experimental data collected for the International Towing Tank Conference (ITTC) headform

are a good example. Cavitation inception indices on this headform ranged from 0.3 to 0.6. Even the appearance of the cavitation varied, some forms looking totally dissimilar from others. It was pointed out by Acosta and Parkin[1*] that boundary layer characteristics and free stream nuclei are responsible for producing the varied appearance of cavitation on a single test model. Sensitivity to air content is also observed in model propeller tip-vortex cavitation experiments. Due to the lack of nuclei, difficulty in producing cavitation in a depressurized towing tank has been observed[2]. With the introduction of bubbles by electrolysis ahead of the propeller, the occurrence of tip-vortex cavitation was significantly enhanced. This fact raises the question "Which cavitation number measured in model tests should be used to scale the prototype inception?"

In the ocean, propeller cavitation inception data from the same class of ships have been known to exhibit a wide range of scatter. The causes are many. However, laboratory studies suggest that environmental effects may contribute partly to the scatter. The understanding of physical phenomena governing the cavitation inception process, especially the influence of cavitation nuclei on bubble bursting, is important for assisting a propeller designer in dealing with cavitation.

In the present investigation, the environmental effects of ocean, lake, and laboratory waters on cavitation were examined. Ocean measurements were conducted at several locations in the early spring of 1983 in Exuma Sound near the Bahamas and the Gulf Stream off the coast of Florida. Lake measurements were conducted in April of 1985 at two locations in Lake Pend Oreille, Idaho. The laboratory measurements were made in the DTNSRDC 12-in. water tunnel to provide a reference for comparison between ocean, lake, and laboratory waters.

The environmental effect on cavitation was measured by a cavitation susceptibility meter consisting of a venturi, a hydrophone, a pressure transducer, and a flow-rate sensor. It is important to remark that the cavitation experiments were conducted *in situ*. Nuclei concentrations and size distributions were measured by a microbubble light detector. Water samples examined by the microbubble detector were obtained from a sample collector which maintained *in situ* water pressure. In the ocean investigation,[3] a full range of other types of oceanographic data was also collected. The range of depth covered in the ocean and lake was 10 to 200 m. Related holographic measurements of cavitation nuclei in the ocean have been reported by O'Hern, J. Katz and Acosta.[4]

Experimental results show the influence of geographic locations and depths on both nuclei distributions and cavitation inception. Bubble instability theory and the Rayleigh-Plesset dynamic equation are used to assist the interpretation of the test results. Conclusions and recommendations are given to complete the report.

*A complete listing of references is given on page 45.

## TENSILE STRENGTH OF A REAL VERSUS AN IDEAL FLUID

Pure liquids at ambient temperature are known to withstand very large tensile stresses before they rupture to form cavities. However, in realistic circumstances a liquid contains weak spots or nuclei, which allow a phase change of the liquid at much lower tensile stresses or even at positive pressures. Cavitation inception indices measured on a lifting body or a headform are known to exhibit a wide range of inception values with respect to the "quality" of the water.

The pressure distribution on a lifting surface can be described by a pressure coefficient,

$$-C_p(x) = \frac{P_0 - P(x)}{(1/2)\,\varrho V_0^2} \tag{1}$$

where $P_0$, $P$, $\varrho$, and $V_o$ are the reference pressure, local pressure on the body surface, fluid density, and the reference velocity, respectively. The symbol x denotes the spatial coordinate in the flow direction. The pressure coefficients are mainly functions of foil geometry and the foil angle of attack.

Cavitation measurements on a body or lifting surface are generally expressed in terms of a cavitation number $\sigma_v$ given by

$$\sigma_v = \frac{P_0 - P_v}{(1/2)\,\varrho V_0^2} \tag{2}$$

where $P_v$ is the vapor pressure of the liquid. It has generally been assumed that cavitation inception occurs when the local pressure falls to or below the vapor pressure of the fluid. One of the main goals in the present investigation is to examine the validity of this assumption.

Cavitation inception on full scale propellers operated at a given depth often occurs at different ship speeds $V_o$. Similarly, for a ship operated at different depths, the measured cavitation inception speeds do not follow strictly the square root of depth or reference pressure relation which follows from Equation (2) above. Thus, there is a large scattering of the inception data at sea. Similar phenomena are found in laboratory cavitation experiments. These observations have led to the hypothesis of cavitation occuring only on specific sites or nuclei.

It is a plausible assumption that cavitation inception occurs at the spot on a body or lifting surface corresponding to the minimum pressure. We can define the cavitation inception index $\sigma_i$ by

$$\sigma_i = -C_{pmin} = \frac{P_0 - P_{min}}{(1/2)\varrho V_0^2} = \frac{P_0 - P_c}{(1/2)\,\varrho V_0^2} \tag{3}$$

where $P_{min}$ is the minimum pressure occurring on the body. If we hypothesize that inception is actually the process of cavitation nuclei blowing up, then $P_{min}$ represents the critical pressure $P_c$ of the weakest nucleus that transits through the low pressure zone. The term $P_c$ reflects the tensile

strength required of a real fluid to have the phase change occur. If $P_c = P_v$, then cavitation inception represents vaporization and the classic cavitation scaling law follows. In general, however, $P_c$ is different from $P_v$. By carrying out cavitation susceptibility measurements in ocean and lake waters, the environmental effects of nuclei on cavitation can be evaluated.

## CAVITATION SUSCEPTIBILITY MEASURING SYSTEM

The device used to measure the cavitation susceptibility of ocean water must be simple to operate and able to produce very low pressures for cavitation at deep depth. Headforms have been used in laboratories for susceptibility measurements.[5,6] However, it is extremely difficult to produce a sufficiently low pressure on a headform to cavitate at deep depths. An orifice is a good cavitator which is very simple in geometry and readily produces low pressures; but the vorticity of an orifice flow includes Reynolds number effects that would be difficult to distinguish from nuclei effects.

A venturi, which satisfies the above requirements with ease, was selected as the cavitator in the present study. Based on the requirement of a smooth surface finish and accurate contour fabrication of the venturi throat, the device recently developed by Lecoffre of Neyretec in Grenoble was selected for the present application. This venturi has a 16:1 area contraction ratio and a throat diameter of 2 mm. Further discussion of this venturi is given in Reference[7].

The cavitation susceptibility measuring system used in the sea and lake has two major components: an underwater unit, which causes and detects cavitation, and a shipboard sub system which controls the underwater unit and conditions data signals for recording and display. The two components are interconnected by a multiconductor cable. Figures 1 and 2 are sketches of this underwater system which is deployed vertically to a designated depth. Sea water is drawn through a filter screen which filters out particles larger than 1 mm that can damage the venturi. The flow then passes through the venturi, the pump, a flow straightener, and finally the flow meter before exhausting to the outside.

The flow rate is regulated by a motor-speed controller in the shipboard subsystem. The cavitation signals are detected by a wideband high frequency hydrophone and then band-pass filtered between 10 and 100 kHz. The acoustic signal is multiplexed with the engineering-sensor data of flow rate and ambient pressure, and together they are transmitted to the shipboard electronics via an electromechanical cable. The signals are then processed on board for display and recording by the shipboard electronics.

The flow-rate sensor, a Flo-Tech Model FSP-375 turbine flowmeter, has an accuracy of $\pm 0.5\%$ of flow rate. The pressure is measured by a Sensotec Model 2988 pressure transducer for 0 to 3.4 bars (0 to 50 psia) and Model 1926 for 0 to 34 bars (0 to 500 psia) with an accuracy of $\pm 0.25\%$ of full scale. The flow meter and the pressure sensors have been independently calibrated at DTNSRDC.

In the 12-in. water tunnel, the same venturi unit was used but the pressure sensors were replaced by mercury and water manometers. A pipe parallel to the water tunnel flow was used to transfer water from the center of the test section to the venturi. A sketch of this circulating system is shown in Figure 3. A major difference between the ocean and the 12-in. water tunnel set-up is that the light-scattering microbubble detector was in-line with the venturi system in the 12-in. water-tunnel experiments, whereas the microbubble detecting system and venturi systems were deployed separately in the ocean and lake experiments.

## MICROBUBBLE AND PARTICLE MEASURING SYSTEM

The nuclei measuring system consists of two major components: an underwater sample collector and a shipboard-light scattering bubble detector. In the water tunnel experiments, only the bubble detector was used. In the ocean and lake, nuclei were measured by examining the microbubbles retrieved from depth in a large sampler. The retrieval device is a 100-L pressure tank with an internal bladder and a large valve at the bottom. After pressurizing the bladder with shipboard nitrogen to the pressure at which the water sample is to be collected, the tank is then lowered to the desired depth. The nitrogen in the bladder bubbles out from a top hose while the ocean water slowly fills the tank through the bottom valve as the bladder collapses. The exit of the top hose is over 2 m above the water intake as seen in Figure 4. The filling is stopped with a residual amount of nitrogen left in the bladder to act as a pressure reservoir.

Upon retrieval to shipboard, the microbubble detector is connected to the bottom valve of the tank and a pressurized nitrogen supply line is connected to the bladder. The 76 to 95 L water sample then exhausts through the detector as the bottom valve is opened and the bladder expands inside the tank. The entire process maintains the ocean water sample at *in situ* pressure until the water sample passes downstream of the detector. A diagram of the device is shown in Figure 4. This device is designed for deep-depth applications.

The size and concentration of microbubbles in the 12-in. water tunnel, and the ocean and lake waters were measured with the same light-scattering bubble detector described by Gowing and Ling.[8] In this device, two rectangular white light beams from an incandescent lamp shine across the water sample that flows through a 3.8-cm I.D. pipe, around which the instrument is built. A diagram of the instrument is shown in Figure 5. Two light beams are used to measure the elapsed time for a bubble to cross between the beams, which yields the bubble's velocity. A series of lenses and masks define the optical-detecting volumes in the center of the pipe, and the light scattered from the bubbles is focused onto photo-multiplier tubes in the receiving optics. The angle of the scattered light uses the specular surface reflection of bubbles to distinguish them from the diffuse reflection of particles. Thus, the device is insensitive to particles if the particulate content is not extremely high.

The voltage pulses from the bubbles are recorded on a Racal tape recorder and then played back through a Nicolet oscilloscope and A/D converter. A PDP-11 computer sorts and counts the digitized pulses and the resultant spectrum is produced. Further discussion on this subject is given by Ling, Gowing and Shen[9]. To evaluate the reliability of the present device for bubble measurements, a comparison test of this device with an in-line holographic camera was carried out at a California Institute of Technology (CIT) water tunnel and reported in a paper by Katz et al[10].

For the 12-in. water-tunnel tests, the bubble detector was connected to a pipe that transferred water from the center of the tunnel test section to the detector and then to the venturi. After flowing 2-m through a 2-cm I.D. rubber hose to the venturi, the water went through a pump and a flowmeter and then back to the tunnel. The pump and flowmeter were the same ones used in the ocean subsystem. Pressure losses in the flow circuit upstream of the venturi were negligible, and the bubbles were measured at a pressure of about 0.1 bar less than the static pressure upstream of the venturi. Also, in the water tunnel tests, the bubbles in the 1- to 2.5-$\mu$m radius range as well as the particles in the 1- to 7-$\mu$m radius range were measured with an Elzone Counter from Particle Data Systems, Inc. The 1- and 2.5-$\mu$m bubble counts were distinguished from the particle counts by examining the nuclei spectra in a batch of water sampled from the water tunnel immediately after the test and then by re-examining after about 2 days to allow the bubbles to rise out.

## OCEANOGRAPHIC DATA MEASURING SYSTEM

Standard oceanographic data were collected on the sea trip as continuous water column measurements made with a Neil Brown conductivity-temperature-depth probe equipped with a transmissometer. A General Oceanics Rosette sampling device collected water samples from discrete depths. The temperature, water density, oxygen content, etc., from the oceanographic data were mapped throughout the ocean tests. Further discussion of the data was recorded by Zsolney,[3] et al. Surface tension measurements were made using a capillary-tube apparatus from the Fisher Scientific Company The water samples used in these tests came from the Rosette sampling device or the microbubble sample collector.

## CAVITATION SUSCEPTIBILITY AND BUBBLE MEASUREMENTS IN THE 12-INCH WATER TUNNEL

The same venturi used in the ocean and lake was used in the 12-in. water tunnel to measure the variation in cavitation susceptibility of laboratory water. The test set-up is shown in Figure 3. The light scattering device used for bubble measurements was also installed in-line with the venturi unit.

Six test results, denoted by WT1 through WT6, are presented in this report. The measured numbers of bubbles per cubic centimeter, N/cm$^3$, for these runs are shown in Table 1. The symbol

$\alpha_{ST}$ denotes the dissolved air saturation relative to 20°C and 1 bar pressure measured by a Van Slyke device. The symbol $\alpha_E$ denotes the same air content but relative to the actual pressure in the tunnel. The symbol $R_0$ denotes the bubble radius.

Because of the large deaerator tank on this tunnel, a factor of 30 difference in the bubble concentrations can be produced. The bubble concentrations and air contents measured at a constant ambient pressure of 1.17 bars are given in Figure 6.

The flow characteristics at cavitation inception, as "called" by a hydrophone, are given in Table 2. The measured mean throat velocity $V_0$, the corresponding Reynolds number Re, the minimum throat pressure coefficient $-C_{pmin}$, the cavitation inception index $\sigma_i$, and the throat pressure $P_T$ at inception are listed here. The negative sign with the throat pressure $P_T$ denotes a compression and a positive sign denotes tension. The first three test runs correspond to supersaturated air content conditions at standard temperature and pressure, and the last three test runs correspond to medium and low air content conditions.

TABLE 1 — WATER TUNNEL BUBBLE CONCENTRATIONS

| Test No. | $\alpha_{ST}$ | $P_o$ (bar) | $\alpha_E$ | $R_o > 10\mu m$ | Bubble Concentration N/cm$^3$ | | |
|---|---|---|---|---|---|---|---|
| | | | | | $R_o > 15\mu m$ | $R_o > 20\mu m$ | $R_o > 30\mu m$ |
| WT1 | 1.05 | 0.5 | 2.10 | 3.6 | 1.0 | 0.32 | 0.08 |
| WT2 | 1.20 | 1.17 | 1.02 | 2.8 | 1.0 | 0.52 | 0.10 |
| WT3 | 1.20 | 1.87 | 0.65 | 1.4 | 0.36 | 0.14 | 0.028 |
| WT4 | 0.60 | 1.17 | 0.53 | — | — | — | — |
| WT5 | 0.50 | 1.17 | 0.42 | 0.39 | 0.18 | 0.10 | 0.020 |
| WT6 | 0.07 | 1.16 | 0.06 | 0.15 | 0.028 | 0.0085 | 0.0011 |

TABLE 2 — MEASURED CRITICAL THROAT SPEEDS AND CAVITATION INCEPTION INDICES IN THE 12-INCH WATER TUNNEL

| Test No. | $\alpha_{ST}$ | $P_o$ (bar) | $\alpha_E$ | $V_0$ (m/s) | $\sigma_i$ | $R_e$ | $-C_{pmin}$ | $P_t$ (Pa) |
|---|---|---|---|---|---|---|---|---|
| WT1 | 1.05 | 0.5 | 2.10 | 8.47 | 1.31 | $1.8 \times 10^4$ | 1.28 | $-0.04 \times 10^5$ |
| WT2 | 1.20 | 1.17 | 1.02 | 13.0 | 1.39 | $2.6 \times 10^4$ | 1.25 | $-0.11 \times 10^5$ |
| WT3 | 1.20 | 1.87 | 0.65 | 19.1 | 1.02 | $3.8 \times 10^4$ | 1.23 | $0.37 \times 10^5$ |
| WT4 | 0.60 | 1.17 | 0.53 | 15.3 | 0.96 | $3.0 \times 10^4$ | 1.24 | $0.28 \times 10^5$ |
| WT5 | 0.50 | 1.17 | 0.42 | 16.3 | 0.86 | $3.3 \times 10^4$ | 1.23 | $0.47 \times 10^5$ |
| WT6 | 0.07 | 1.16 | 0.06 | 21.6 | 0.48 | $4.3 \times 10^4$ | 1.22 | $1.69 \times 10^5$ |

Consider the test series consisting of runs WT2, WT4, WT5 and WT6. These four test runs were conducted at the same test pressure. The bubble concentrations in terms of air contents are given in Table 1 and plotted in Figure 6. The decrease in bubble concentration with air content is evident. The measured cavitation index $\sigma_i$ varied from 0.48 at an extremely low air content to 1.38 at the super-saturated conditions. A dramatic change in $\sigma_i$, of almost a factor of three, was measured. A large variation in $\sigma_i$ with air content and bubble distribution has also been observed in headform measurements[9].

From the series of 12-in. water tunnel tests, the following observations are made:

1. A factor of 30 difference in the bubble concentrations can be produced.
2. The bubble size distributions and inception indices follow air contents in a systematic pattern.
3. Depending on the bubble concentrations, $\sigma_i$ can vary by a factor of three. Such a large variation in $\sigma_i$ makes bubble cavitation scaling from model to prototype difficult without taking nuclei into account.
4. The venturi used in the present program can detect relative changes in bubble concentrations by its indication of different $\sigma_i$ values. The variation of $\sigma_i$ with bubble concentration is systematic.
5. The measured water tensile strength of 0.3 to 1.7 bars is compatible with the values measured by Knapp.[11]

## OCEAN MEASUREMENTS

Sea measurements were carried out in Exuma Sound and the Gulf Stream near the coast of Florida to provide comparable susceptibility results in natural bodies of water. To investigate the effect of depth on susceptibility, measurements were made at depths from 10 to 200 m. The cruise track and station locations are shown on the map of Figure 7. The cruise took place between 25 March and 5 April, 1983.

Station 1 was designated as the "shake down" station to check the instrumentation. Station 2 was used to tune the instruments. The data from these two stations were not used in this report. Susceptibility measurements covered Stations 3 to 6 in Exuma Sound, and 7 to 9 in the Gulf Stream in the Straits of Florida. Station 6 was the same location as Station 3 but 4 days later. Because of the strong current and ship drift in the Gulf Stream, difficulties were experienced in obtaining deep depth data there. However, with good weather throughout the whole test program, the fluctuations in surface elevation were relatively small and the ambient pressures seen by the pressure sensors were almost constant at a given depth.

The sequence of data collection follows. Once on station, the Neil Brown conductivity-temperature-depth probe equipped with a transmissometer was used to collect standard oceanograhic data. This was followed by the deployment of the General Oceanics Rosette sampling device to collect

water samples from discrete depths. All of the oceanographic tests took only 2 to 3 h/station. Immediately after the completion of the oceanographic tests, the cavitation susceptibility meter was deployed.

The underwater venturi unit was deployed to a specified depth while monitoring the pressure on the transducers. Cable markers provided general guidance on the overall depth. Once at depth, the flow rate was set just below the critical speed such that no acoustic signals were detected for 3 to 5 min. The flow was then gradually increased until high amplitude acoustic signals were detected, and then tuned to attain a specific frequency of cavitation events. The flow rate, ambient pressure, and acoustic signals were recorded on tape and displayed on the shipboard readout unit for 3 to 5 min, with a few 10 min runs.

Except at Station 6, three flow rates corresponding to three different frequencies of cavitation events were measured at each depth. It took approximately 3 h to complete cavitation susceptibility measurements at one station. The microbubble and particle measurements then followed. The deployment and retrieval of the water sample collector and the measurements of nuclei distributions by the light scattering device consumed a lot of time. This limited the data on nuclei distribution.

## OCEANOGRAPHIC MEASUREMENTS

The temperature, water density, and dissolved oxygen distributions relative to 1-bar pressure are given in Figures 8, 9 and 10 as a function of depth. (The other important oceanographic data such as nitrogen, salinity, carbon, and biological parameters etc. are given and discussed in Reference 12.) In the ocean, the biological parameters such as photoplankton, zooplankton and living cell distributions etc. may play a role in cavitation. Nevertheless, the evaluations in this report are limited to relating cavitation to bubble measurements.

The water temperature distribution is shown in Figure 8. The temperature near the surface was about 24°C and dropped to 21°C at 200-m depth in Exuma Sound. In the Gulf Stream, the temperature at the surface was about 25°C and dropped to 15°C at 200-m depth.[3] The influence of geographic locations on water temperature was very small in Exuma Sound during the tests. On the other hand, the water temperature in the Gulf Stream showed significant variation with geographic locations. The thermoclines in Exuma Sound occurred at around 150-m deep and in the Gulf Stream at around 75 to 100-m deep (see Figure 9).

The dissolved oxygen distribution in Exuma Sound was relatively insensitive to geographic location (Figure 10). Furthermore, the percent of oxygen saturation dropped very gradually with increases in water depth. At the surface, the water was about 100% saturated with oxygen. Even at 200 m, 83% saturation was measured in Exuma Sound. On the other hand, the oxygen saturation distribution in the Gulf Stream was very different. The percent of saturation decreased markedly at depths greater than 100 m. At 200 m, a value of less than 50% saturation was measured.[3] The significance of this

parameter, "dissolved oxygen", is that quite often biological activity is related to oxygen balances and microbubble distributions may well be a consequence of biological activity.

The surface tension of the ocean and lake waters was measured using a capillary device from Fisher Scientific Co. The device consists of a 0.5-mm diameter borosilicate glass capillary tube, graduated from 0 to 10 cm in 1-mm increments. Using a reading glass, the distance between the lower meniscus in the outer tube and the upper meniscus in the capillary tube gives the surface tension. In the ocean, the water sample was taken from the microbubble sample collector or the Rosette Sampling device. The test results, not given in this report, showed that the surface tension of the sea water was invariant throughout the test within the accuracy of measurement. The same was true with Lake Pend Oreille water.

## MICROBUBBLE MEASUREMENTS

The size and concentration of microbubbles in the 12-in. water tunnel, the ocean, and the lake were measured with the same light scattering bubble detector. The ocean and lake microbubble spectra were measured by examining the microbubbles retrieved from depth in the large water sampler, and the measurements were then carried out on shipboard. However, it is important to point out that the entire sampling process maintained the ocean water sample at *in situ* pressure until the sample passed downstream of the bubble detector. Because of the time involved in the deployment and retrieval of the sample collector, the number of microbubble measurements is relatively limited compared to the cavitation measurements.

From the nuclei measurements on board the container ship "Sydney Express" and other oceanographic investigations, Weitendorf[13] found that a great number of cavitation nuclei are always present in the ocean. Experiments by Medwin[14] in coastal waters indicate that bubbles with radii between 15 and 200 $\mu$m are present to depths of 40 m.

The ocean microbubble measurements at the 10-m depth are given in Figure 11. The same data are replotted in Figure 6 for comparison with the water-tunnel data. The ocean bubble concentrations fall between those corresponding to supersaturation and medium air content conditions for the water tunnel. Note that these laboratory bubble measurements were at 1.17 bars ambient pressure while the ocean data were measured at 2.09 bars. The difference in bubble size because of these pressure differences would be about 21%. Because of the significant effect of ambient pressure on microbubble instability, however, the comparison given in Figure 6 can only be interpreted qualitatively. The nuclei size distributions with depth in Exuma Sound and the Gulf Stream are given in Figure 12.

The existence of gas bubbles near the ocean surface, down to 40 m, has been well documented[15]. But, the existence and persistence of gas bubbles at deep depths of 200 m has not been previously reported. Gas absorption physics would predict rapid absorption of bubbles at these depths and low

relative air saturation levels. For this reason, it is felt that the word "nuclei" may be more proper than the word bubble to describe the light scatterers detected at the deep depths. It is quite possible that in addition to gas bubbles, cavitation nuclei can consist of organic matter such as plankton or other microscopic biological matter that serves as a discontinuity in water. Nevertheless, most of the signals seen on the oscilloscope during the ocean-water measurement resembled those of bubbles measured in laboratory water. The possible existence of gas bubbles at deep depths is therefore strongly suggested. This is a very important result. Further work should be carried out to verify it, perhaps by a holographic or photographic device in parallel with the present set-up.

The bubble concentrations in the Gulf Stream are greater than those in Exuma Sound (see Figure 12). This correlates with biological activity which also was greater in the Gulf Stream than in Exuma Sound. In both bodies of water, the nuclei concentration for a given bubble size decreased with deeper depths. However, the rate of decrease seems steeper in the Gulf Stream than in Exuma Sound. For example, at 150 m, the measured nuclei concentrations in Exuma Sound are greater than those in the Gulf Stream. This observation is consistent with the oceanographic measurements, namely that the oxygen saturation measurements given in Figure 10 show a similar trend. The slope of the bubble concentrations as a function of bubble size is similar to the size-concentration distributions found by other investigators for bubbles in water tunnels or the ocean. This consistency of the shape of the bubble distributions at various sites has been previously noted.[10]

No attempt is made here to rationalize why nuclei populations are different at the two ocean locations. In the next section, however, an attempt will be made to correlate the measured nuclei and the cavitation measurements.

## CAVITATION MEASUREMENTS

Two types of acoustic signals were detected in the cavitation measurements. The first, due to single and multiple bubble bursting in the venturi throat away from the venturi wall, appeared on an oscilloscope as a signal that rose very sharply above the background noise level and then decayed gradually. If bubble bursting took place near or on the venturi wall, as in surface sheet cavitation, the second type of signal resulted. This signal rose quickly and persisted at the same level. The acoustic intensity of the surface cavitation was much higher than that of the background noise but significantly lower than that of the single bubble bursting. For the cavitation susceptibility study, only cavitation from a single bubble or multi-bubble bursting was of interest. Surface sheet cavitation did occur in the venturi occasionally but it was easily removed by reducing the throat velocity. Increasing the throat velocity again usually did not restart the surface cavitation.

The background noise of the acoustic channel was about 100 mV peak-to-peak. The bursting noise of a cavitation bubble was generally a few volts or more; hence the signal to noise ratio was

much greater than 10. As a result, it was not difficult to detect cavitation bursting acoustically. To determine the frequency of cavitation events, a threshold of 1 V was set as the trigger to count cavitation bursting in the counter. The oscilloscope trace indicated that the rebound of the bubble bursting was less than 1 ms. To distinguish the bursting of multibubbles from the rebound signals of a single bubble, a time lapse of 1.5 ms was set to trigger the counting of another event. Typical acoustic signals of a single bubble bursting .re shown in Figure 13.

The test matrix at Station 6 was more extensive than at other stations. The measured frequency of cavitation events and flow rates at Station 6 are shown in Figure 14 at four depths. The vertical axis shows the averaged frequency of cavitation events per minute for a typical test run of 3 to 5 min. The horizontal axis gives the corresponding flow rate measured in the middle of the test run. Plots are shown for water depths of 75, 100, 125 and 150 m, respectively. Note that as the ambient pressure increases with depth so does the required flow rate to induce cavitation.

Laboratory experiments indicate that the occurrence of bubble cavitation is related to the available nuclei content which is not uniformly distributed in space. In a separate report under preparation, the nuclei distributions measured in the ocean and laboratory are found to follow a Poisson distribution within a 95% confidence level. This fact has also been reported by Lecoffre, et al., for laboratory water.[15] Consequently, the frequency of cavitation events per unit time at a given flow rate should also be Poisson distributed. Occasionally, a small increase in flow rate produced a lower frequency of cavitation events as seen in Figure 14, but overall, the general trend is very clear. At a given depth or ambient pressure, there existed a critical flow rate below which no cavitation was detected. For a flow rate greater than this critical value, a slight increase in flow rate resulted in a significant increase in the frequency of cavitation events.

To investigate the influence of different venturis on cavitation, the first venturi was replaced by a second venturi. Both venturis were purchased in the same lot from Neyretec in Grenoble. Cavitation susceptibility measurements were carried out at a 25-m depth at Station 6. The test results are shown in Figure 15. The first venturi is denoted as Venturi 1. and the second as Venturi 2. Due to a slight difference in ambient pressure between these two test runs, the nondimensional cavitation number is used for comparison. Both venturis gave the same trend. This result adds to the confidence in the test data. To add a remark, the original Venturi 1 was reinstalled in the cavitation susceptibility meter and used in the subsequent tests in the Gulf Stream and Lake Pend Oreille.

For completeness, the cavitation frequency versus flow rates for Stations 3, 4, and 5 in Exuma Sound and 7 and 9 in the Gulf Stream are given in Figure 16. The same conclusion obtained previously can also be made from Figure 16, that, at a given depth, there existed a critical flow rate below which no cavitation bursting was detected. A slight increase in flow rate beyond the critical value produced a

large increase in the frequency of cavitation events. The question arises whether this is a real fluid phenomenon or an intrinsic property of the venturi that was used as a cavitation generator.

As mentioned previously, the existence of gas bubbles down to 40 m has been well documented. Bubble dynamic theory should be applicable to investigation of cavitation events at least down to a 40-m depth. Based on the Rayleigh equation, bubble instability curves have been constructed and are given in Figure 17. The effect of the pressure drop due to viscous losses in the venturi throat has been included. Further discussions are given in Reference.[17]

The free parameter in Figure 17 is the ambient pressure $P_0$. The bold line is a special case corresponding to the 10-m depth pressure of 2.09 bars. The horizontal axis corresponds to bubble size. The vertical axis corresponds to the critical velocity at which the bubble becomes unstable. The curves are referred to as static bubble instability curves. Similar figures of bubble instability have been computed by d'Agostino and Acosta assuming potential flow.[18] In the case of Figure 17, for bubbles larger than 7 $\mu$m, the curve is almost flat. For bubbles smaller than 7 $\mu$m, a substantial increase in throat velocity is needed for small bubbles to become unstable.

Figure 17 clearly shows that at a given depth or ambient pressure there exists a critical velocity below which all the bubbles are stable and bubble cavitation would not be expected to occur. When the critical velocity is reached, all the bubbles greater than 7 $\mu$m become unstable and a large number of bursting bubbles is expected. Different cavitators would have different critical velocities, but the general characteristics of instability curves should remain the same. This instability theory supports the idea that the sudden increase in cavitation frequency with flow rate is a consequence of bubbles becoming unstable and hence this is a real fluid phenomenon. Even though the existence of micro-bubbles at deep depths has not been proved conclusively, the same cavitation frequency trends observed in Figure 16 occurred at the deep depths, which supports the possible existence of bubbles.

The measured cavitation inception indices in Exuma Sound and the Gulf Stream are given in Figures 18 and 19, respectively. The corresponding geographic stations have been given in Figure 7. Cavitation inception must be defined here. Although the definition of cavitation inception is subjective, it is simply assumed in this report that cavitation inception occurs when the bursting signals are detected at an average frequency of 10 events per minute. (0.17 events per second.) The corresponding flow rate is called the critical flow rate $Q_i$ and the mean throat velocity $V_i$ is called the critical throat velocity. The cavitation inception index $\sigma_i$ is defined as

$$\sigma_i = \frac{P_0 - P_v}{(1/2)\,\varrho V_i^2} \tag{4}$$

Basically Equation (4) is the same as Equation (2). The only difference is that the critical throat velocity instead of free stream velocity is used for normalization. The curve denoted by $C_{pmin}$ in

Figures 18 and 19 corresponds to the measured minimum pressure coefficient on the venturi surface at different Reynolds numbers.

From Figures 17, 18, and 19, the following observations can be made:

1. There was no difficulty to induce *in situ* cavitation throughout the test matrix, even down to 200 m; hence, deep ocean water cavitates readily.

2. At 10 m, the values of $\sigma_i$ exhibit a large variation with geographic location. They range from 0.92 to 1.16 in Exuma Sound among 4 stations and 1.13 to 1.24 in the Gulf Stream. A relatively large variation in $\sigma_i$ was also observed at 25 m.

3. At 75 m, the measured values of $\sigma_i$ at 4 stations ranged from 1.17 to 1.21 in Exuma Sound. The total variation of $\sigma_i$ among these stations is within 3%. The same statement holds true at depths greater than 75 m. Cavitation nuclei populations were also similar between stations in Exuma Sound, at least at depths greater than 75 m. This indicates that the venturi meter responds to similar nuclei concentrations reasonably well and that similar nuclei populations yield similar cavitation results.

4. In Exuma Sound, the average value of $\sigma_i$ among 4 stations increased at 200 m. This trend was not originally expected and cannot be currently explained.

5. In the Gulf Stream, the peak value of $\sigma_i$ was measured at 100 m and $\sigma_i$ decreased at deeper depths. This trend is opposite to the one noted for Exuma Sound.

6. In Exuma Sound, $\sigma_{max} = 1.26$ was measured at 200 m and $\sigma_{min} = 0.92$ was measured at 10 m. This gives a total variation in $\sigma_i$ of 37%. Below 25 m, the lowest value of $\sigma = 1.16$ was measured at 75 m depth. This gives a total variation in $\sigma_i$ of 9% between 75 to 200 m.

7. In the Gulf Stream, $\sigma_{max} = 1.28$ was measured at 100 m, and $\sigma_{min} = 1.15$ was measured at 200 m. This gives a total variation in $\sigma_i$ of 12% between 75 to 200 m.

8. Between 10 and 100 m of depth, $\sigma_i$ is higher overall in the Gulf Stream than in Exuma Sound. Hence, the Gulf Stream is seen to be more susceptible to cavitation than Exuma Sound. At depths greater than 100 m, the opposite is true.

9. A comparison of $\sigma_i$ measured between the ocean and the 12-in. water tunnel indicates that high air contents are needed in the laboratory to produce the same cavitation susceptibility as the ocean. This point will be further amplified in the following theoretical studies.

## THEORETICAL INTERPRETATION

It is the purpose of this section to see whether some theories can be used to interpret some of the test results. Water tunnel data show that gas bubbles produce cavitation bursting in the venturi throat. It is assumed that both static and dynamic bubble theories are therefore applicable to the present study.

At shallow depths the Gulf Stream was seen to be more susceptible to cavitation than Exuma Sound. At deep depths the opposite trend was noticed. Microbubble measurements shown in Figure 12 give higher bubble concentrations in the Gulf Stream than in Exuma Sound at shallow depths, and the opposite at deeper depths. Cavitation data are thus supported by nuclei measurements. This result compliments the water tunnel data for which cavitation was very closely related to the concentration of cavitation nuclei.

One of the unexpected results is the increase in $\sigma_i$ with depth in Exuma Sound. Another unexpected result is that variation of $\sigma_i$ among 4 stations is significantly greater at a 10-m depth than say at a 100-m depth, while the measured nuclei as seen in Figure 12 are more abundant at shallow depth than at deep depth. It was anticipated that $\sigma_i$ would vary more with sparser nuclei populations than abundant ones. Furthermore, the measured $\sigma_i$ value greater than 1.0 was not expected.

In a recent paper by Shen, Gowing and Pierce,[17] bubble instability curves, in terms of the ambient pressure, were computed and they are repeated here in Figure 17. The curve denoted by 2.09 bars corresponds to an ocean depth of 10 m. The curve is almost flat for bubble sizes $R_o$ greater than 7 $\mu$m. With only a minute increase in throat velocity, all bubbles greater than 7 $\mu$m will become unstable, and this radius is termed the critical radius. The locus of critical bubble radii is also shown in Figure 17.

The critical radii are seen to decrease significantly with an increase in ambient pressure or depth. For example, the critical radius is seen to be around 0.4 $\mu$m at 200 m deep (21.7 bars). All bubbles greater than 0.4 $\mu$m would then be candidates for cavitation bursting. Recall that the bubble concentration drops almost linearly with increasing bubble size on a logarithmic scale. Consequently, the concentration of bubbles eligible to cavitate can theoretically increase with depth if the plots in Figure 12 can be extrapolated to smaller sizes. This may explain the fact that $\sigma_i$ increases with depth as it did in Exuma Sound. Because the relatively large bubbles measured by the detector would only form a small fraction of the total bubbles eligible for cavitation if the plots in Figure 12 were extrapolated, this hypothesis may not be proved as the direct measurement of bubble sizes less than 5 $\mu$m has not successfully been made.

The cavitation inception index $\sigma_i$ defined in Equation (4) is based on the mean venturi throat velocity when the occurrence of bubble bursting was detected. According to potential flow theory, $\sigma_i$ should not be greater than unity. Ocean measurements given in Figures 18 and 19 show otherwise. The viscous effect of a real fluid is seen to play an important role in cavitation susceptibility measurements. This subject has recently been studied by Chahine and Shen,[19] and Shen and Gowing.[20] As flow passes through the venturi throat there will be an energy loss because of the viscous effect. Furthermore, the boundary layer grows and the potential core in the throat shrinks. This results in an accelerating flow in the potential core along the throat. The velocity in the potential core will be substantially higher than the mean throat velocity.

The measured pressure distribution along the venturi throat is given in Figure 20. Because of the energy loss, the pressure coefficient based on the mean throat velocity is seen to be substantially higher than unity. This fact explains why the measured $\sigma_i$ from the ocean can be higher than unity.

The minimum pressure coefficient in the throat occurs at the exit and is shown in Figure 20. The measurements show a 20 to 30% energy loss, which is about the value given by Schlichting in a pipe flow.[21] The minimum pressure coefficients $-C_{pmin}$ corresponding to different flow rates at different depths are plotted in Figures 18 and 19 along with the cavitation data. By comparing the measured $\sigma_i$ and $-C_{pmin}$, some of the test data are seen to coincide with the classic assumption that $P_{min} = P_v$ at the state of cavitation inception. On the other hand, a significant portion of test data shows the noticeable error induced by the classic assumption.

## CAVITATION SUSCEPTIBILITY MEASUREMENTS IN A LAKE

Lake measurements were carried out at Lake Pend Oreille in Idaho at the end of April 1985 to provide results comparable with ocean and laboratory measurements. The hydrophone, flow meter and electric cable used in the ocean cruise had been replaced with new units. The measurements covered two locations. The first station was located next to a yellow barge, and the second station next to a deep mooring. The geographic locations of these two stations are shown in Figure 22.

An expendable Bathythermograph System was used to profile the lake temperature. The temperature measurements were made next to the deep mooring. The temperature was found to remain within 5.6°C of the surface temperature down to 100 m deep. Surface tension measurements yielded values for the lake that were, within instrument accuracy, the same values as for the ocean.

Microbubble and particle measurements were conducted in September of 1984 and April of 1985. Due to some technical problems associated with the water sample collector, the April data are not yet available. For reference purposes the September 1984 data are given in Figure 23.

A comparison of Figures 12 and 23 indicates that more nuclei were measured in the lake than in the ocean. This result was not expected. However, the ocean water was more clear than the lake water because the sampler device could be seen at deeper depths in the ocean than in the lake. A substantial amount of particles included in Figure 23 is suspected.

Cavitation data are shown in Figures 24 and 25. Again, a threshold or critical flow rate required to produce cavitation is evident. The following observations can be made through a comparison of Figures 18, 19 and 25.

1. At 10 m, the values of $\sigma_i$ are 1.05 and 1.26, respectively. These values are similar to those measured in the Gulf Stream and are higher than those measured in Exuma Sound.

2. At 100 m deep, the measured $\sigma_i$ are 1.07 and 1.08 in the lake, 1.23 and 1.28 in the Gulf Stream, and 1.18 to 1.21 in Exuma Sound. Lake water is seen to be less susceptible to cavitation than ocean water at that depth.

3. At 200 m deep, the measured $\sigma_i$ is 1.14 at the lake, 1.15 in the Gulf Stream, and 1.20 to 1.26 in Exuma Sound. The difference between the lake and Exuma Sound can be as high as 12%.

In summary, lake measurements indicate that there would be no difficulty in producing bubble cavitation at 100- and 200-m depths. However, it was found that the flow rates required to induce cavitation were higher at Lake Pend Oreille than at Exuma Sound.

The discussions so far are centered on the cavitation inception index and nuclei distribution. Acoustic intensity generated by the bubble bursting has also been briefly investigated. One noticeable distinction between ocean and lake data is that the acoustic intensities measured in the lake at 150- and 200-m depths were significantly lower than those measured at the shallow depths. This phenomenon was not observed in the case of the ocean measurements. The reason for different acoustic signals in the two different bodies of water is not clear.

## TENSILE STRENGTH DERIVED FROM VENTURI MEASUREMENTS

At a given depth the flow rate required to induce cavitation differs among ocean, lake and laboratory waters. No direct measurements were made to determine the corresponding tensile strength at cavitation inception. Nevertheless, it may be estimated by the following indirect method. The tensile strength $P_t$ is computed by

$$P_t = - P_0 + K \cdot \frac{\varrho}{2} \cdot V_i^2 \tag{5}$$

The negative sign on the right hand side is used to yield positive values for tension and negative values for compression. The symbol K includes the loss coefficient due to viscosity. The actual value of K depends on the venturi geometry and the friction coefficient. In this study, it is approximated by the measured value of $-C_{pmin}$.

The computed tensile strengths of laboratory water at different air contents are given in Table 2. At supersaturation conditions, compression was measured at the state of cavitation inception. At lower air contents and bubble populations, the tunnel water showed tension at inception. A tensile strength of 1.69 bars, corresponding to 24.5 psi was computed at the 7% air content. As shown in Table 2, the range of tensile strengths computed for the 12-in. water tunnel is in the same range as those measured by Knapp at the California Insitute of Technology.[11]

The computed tensile strengths of the ocean and lake waters are given in Tables 3 and 4, respectively. The magnitudes of tensile strength measured in the ocean waters are compatible with those of

laboratory water. The compression computed for the 200-m depth in Exuma Sound was not expected. Further studies are being made to investigate this phenomenon. As a remark, susceptibility works by Crump[22,23] and Knapp[11] also showed large compression in some of their test measurements.

The critical pressure data obtained at sea by the U.S. Navy[17] and French Navy[24] are summarized in a recent report of the 18th ITTC Cavitation Committee and given in Table 5. It is noted that the data given in Reference 16 only cover the depths of 10 and 25 m. The tensile strengths measured near the Mediterranean and Britanny coasts were found to be higher than the values in the Gulf Stream, and less than the values in the Exuma Sound. The existence of tension at the state of cavitation is evident.

The tensile strength computed by Equation (5) does account for the energy loss due to viscosity by using the measured $-C_{pmin}$ value to substitute the value of K. However, the influence of boundary layer growth and potential core acceleration in the throat are not considered. Hopefully, this correction is not large. Further refinements of the theoretical analysis are needed to improve values given in Tables 2, 3, and, 4.

## CONCLUSIONS

For the first time, cavitation susceptibility and nuclei distributions were measured in ocean, lake, and laboratory waters. The depths covered in this test program ranged from 10 to 200 m. To provide a reference for comparison, the water in the 12-in. water tunnel was measured with the same devices used in both ocean and lake.

The important results obtained from the ocean measurements can be summarized as follows:

1. In the Gulf Stream, the water temperature and oxygen distributions were found to vary significantly with change in depth and geographic location. In Exuma Sound, they were less sensitive to change in depth and geographic location.

2. Measured nuclei populations decrease with increased depth. The rate of decrease of nuclei population with depth is qualitatively indicated by the oxygen levels.

3. Correlation between nuclei concentrations and cavitation inception indices was observed. At depths of less than 100 m, bubbles were more abundant in the Gulf Stream than in Exuma Sound, and cavitation was found to occur more easily in the Gulf Stream than in Exuma Sound. At depths deeper than 100 m, there were more nuclei in Exuma Sound than in the Gulf Stream, and cavitation was found to occur more easily in Exuma Sound.

4. Depending on the nuclei populations, variations of cavitation inception indices with depth can take different forms in different bodies of water, as noted in Exuma Sound, the Gulf Stream, and (as noted in the following paragraph) Lake Pend Oreille.

TABLE 3 — TENSILE STENGTH OF OCEAN WATER EXUMA SOUND
(SPRING 1983)
Tensile Strength (bar)*

| Station \ Depth | 10m | 25m | 75m | 100m | 125m | 150m | 200m |
|---|---|---|---|---|---|---|---|
| 3 | 0.73 | 0.76 | 0.37 | 0.08 | 0.01 | 0.06 | −0.58 |
| 4 | 0.46 | 0.47 | 0.44 | 0.27 | 0.43 | −0.08 | −1.11 |
| 5 | 0.64 | 0.17 | 0.36 | 0.28 | 0.32 | 0.51 | −0.28 |
| 6 | 0.11 | 0.55 | 0.07 | 0.02 | 0.19 | 0.21 | 0.07 |
| GULF STREAM (SPRING 1983) | | | | | | | |
| 7 | 0.21 | 0.20 | −0.43 | −0.90 | 0 | 0.35 | 1.04** |
| 8 | 0.19 | 0.54 | 0 | 0.10 | | | |
| 9 | 0.23 | 0.24 | −0.37 | −0.29 | 0.11 | | |

*Negative sign denotes compression.
**Cavitation inception obtained from 10 cavitation events per minute.

TABLE 4 — TENSILE STRENGTH OF LAKE PEND OREILLE
(SPRING 1985)
Tensile Strength (bar)*

| Station \ Depth | 10m | 25m | 50m | 100m | 150m | 200m |
|---|---|---|---|---|---|---|
| 1 | 0 | 0.11 | 0.73 | 1.38 | 1.01** | |
| 2 | 0.35 | 0.40 | 0.74 | 0.16 | 0.77 | 1.08 |

*Negative sign denotes compression.
**Cavitation inception obtained from 10 cavitation events per minute

TABLE 5 — CRITICAL PRESSURE MEASURED AT SEA BY VENTURI METHOD
(TAKEN FROM 18th ITTC CAVITATION COMMITTEE REPORT)

| Station | | Depth (m) | Ambient $P_0$ (bar) | Critical $P_c$ (bar) | R equivalent[2] ($\mu$m) |
|---|---|---|---|---|---|
| Straits of Florida*,17 | A | 10 | 2.09 | 0.21 | 1.47 |
| | | 25 | 3.73 | 0.27 | 1.07 |
| | B | 10 | 2.07 | 0.31 | 1.13 |
| | | 25 | 3.70 | 0.38 | 0.85 |
| | C | 10 | 2.08 | 0.21 | 1.47 |
| | | 25 | 3.69 | 0.31 | 0.98 |
| Bahama Coast*,17 | D | 10 | 2.09 | 0.84 | 0.53 |
| | | 25 | 3.75 | 0.83 | 0.47 |
| | E | 10 | 2.14 | 0.64 | 0.65 |
| | | 25 | 3.77 | 0.55 | 0.65 |
| French Mediterranean Coast (Summer)[24] | | 10 | 2.12 | 0.50 | 0.79 |
| | | 25 | 3.40 | 1.47 | 0.31 |
| | | 30 | 4.17 | 1.33 | 0.32 |
| Britton Coast[24] | A (Winter) | 10 | 2.00 | 0.30 | 1.16 |
| | | 25 | 3.50 | 0.13 | 1.74 |
| | | 35 | 4.43 | 0.19 | 1.28 |
| | B (Spring) | 10 | 1.97 | 0.69 | 0.62 |
| | | 20 | 2.96 | 0.50 | 0.73 |
| | | 30 | 3.90 | 0.10 | 1.97 |
| | | 50 | 5.94 | 1.87 | 0.23 |
| | | 65 | 7.30 | 2.10 | 0.20 |

*Cavitation inception based on zero events per minute in cavitation count.

5. Bubble dynamic and static instability theories show that, given an ambient pressure and speed, there exists a critical minimum bubble radius for cavitation bursting to occur. The sudden appearance of cavitation with increasing speed is borne out by the measurements.

6. The unstable bubble population may actually increase with depth. This idea may be used to explain why cavitation inception indices are higher at deep depths than at shallow depths in Exuma Sound.

7. In Exuma Sound $\sigma_{max} = 1.26$ was measured at 200 m and $\sigma_{min} = 0.92$ was measured at 10 m. Thus, a total variation in $\sigma_i$ of 37% was observed.

8. In the Gulf Stream $\sigma_{max} = 1.28$ was measured at 100 m and $\sigma_{min} = 1.15$ was measured at 200 m. This gives a variation of 12% of $\sigma_i$ between 100 to 200 m.

9. The classic assumption of $P_{min} = P_v$ at the state of cavitation inception can be seriously in error, as noted by the difference between measured values of $\sigma_i$ and $-C_{pmin}$.

The following summary can be made of the lake measurements:

1. More nuclei were measured in the lake than in the ocean. This was not originally expected.

2. Particle measurements indicate that nuclei measured in the lake may consist of a substantial amount of particles. This fact was supported by the observation of reduced visibility of the sample collector at shallow depths, relative to the ocean visibility, and further supported by the light transmission measurements taken with a transmissometer.

3. At the shallow depths of 10 and 25 m, cavitation inception indices measured at the lake are compatible with the Gulf Stream measurements and slightly higher than the values measured at Exuma Sound.

4. At depths greater than 25 m, the lake water was found to be less susceptible to cavitation than in Exuma Sound.

5. At a 200 m depth, the measured value of $\sigma_i$ is 1.14 in the lake, 1.15 in the Gulf Stream, and 1.20 to 1.26 in Exuma Sound. The difference in $\sigma_i$ between the lake water and Exuma Sound water can be as high as 12%.

The important results obtained in the 12-in. water tunnel can be summarized as follows:

1. Because of the deaerator, a factor of 30 difference in the bubble concentrations can be produced.

2. The bubble concentration and size distributions follow the air contents in a systematic way.

3. Depending on the bubble concentrations, $\sigma_i$ varied from 0.49 to 1.38. This is almost a factor of 3 in $\sigma_i$ variation and makes cavitation scaling from model to prototype difficult.

4. A comparison with the ocean measurements indicates that high air contents are is needed in water tunnels to produce the same cavitation inception index as measured in the ocean at deep depths.

5. From bubble dynamics and static instability theories, a critical bubble radius, strongly dependent on pressure and velocity, may be computed. At deep depths and high ambient pressures, the population of unstable bubbles can become very large. The bubble instability theory seems to suggest that the cavitation scaling problem can be significantly minimized by testing the model at high ambient pressures and high test speeds.

## RECOMMENDATIONS

Many important results have been obtained in this test program. Further work is recommended to improve the level of confidence of cavitation susceptibility predictions. It must be noted that the conclusions given in the previous section have been based on limited test data. The influence of seasonal variation and different geographic locations on cavitation should be further investigated.

Lake data clearly show that additional nuclei measurement devices, such as holography,[4] may have to be used in line with the present measuring system so that particles and gas bubbles can be distinguished in nuclei population counts. Further improvements are needed to enhance flow-rate regulation and eliminate flow-rate fluctuations.

The importance of micro-organisms such as zooplankten and their influence on cavitation inception has not been investigated in the present report.

The importance of viscous effects on cavitation measurements by a venturi system has been partially investigated. More theoretical work is needed to separate the viscous effects from nuclei effects.

The report so far is concerned with the effect of nuclei on cavitation inception. The effect of different nuclei on the acoustics of cavitation has not been included.

The present study uses a venturi device as a cavitator. Analytical works are recommended to interpret results obtained in the venturi relative to vortex-type cavitation.

Finally, the present work shows a qualitative correlation between nuclei measurements and cavitation. As pointed out in recent ITTC and ATTC reports, guidance to relate nuclei distributions and cavitation testing procedures in laboratories is needed. This is an area that requires further investigation.

## ACKNOWLEDGMENTS

The authors express their deep appreciation to Dr. A. Zsolnay at NORDA for his support of the sea cruise, and to Mr. D. Gerzina at DTNSRDC for his support of lake measurements. The continuous support and encouragement of Mr. J. H. McCarthy and Dr. F. B. Peterson throughout the course of this project are greatly appreciated. Finally, the benefits of technical discussions with Dr. T.T. Huang are greatly appreciated.

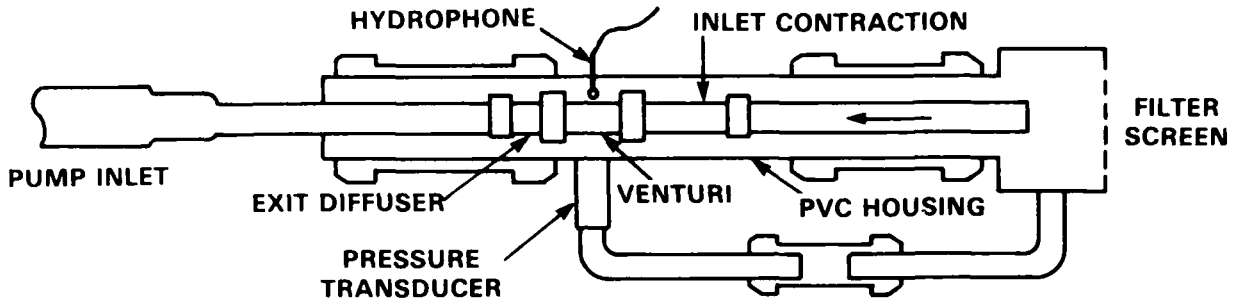


Figure 1 — Cavitation System



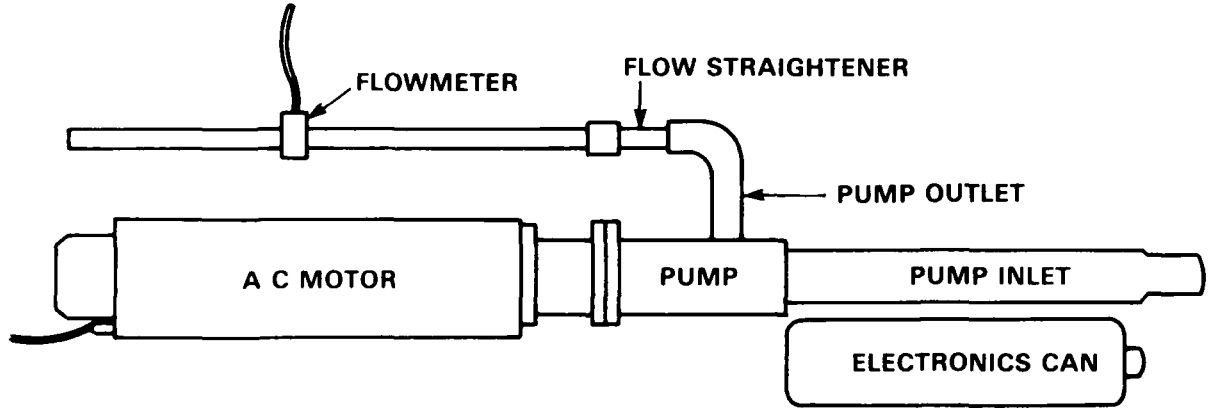


Figure 2 — Motor-Pump Assembly

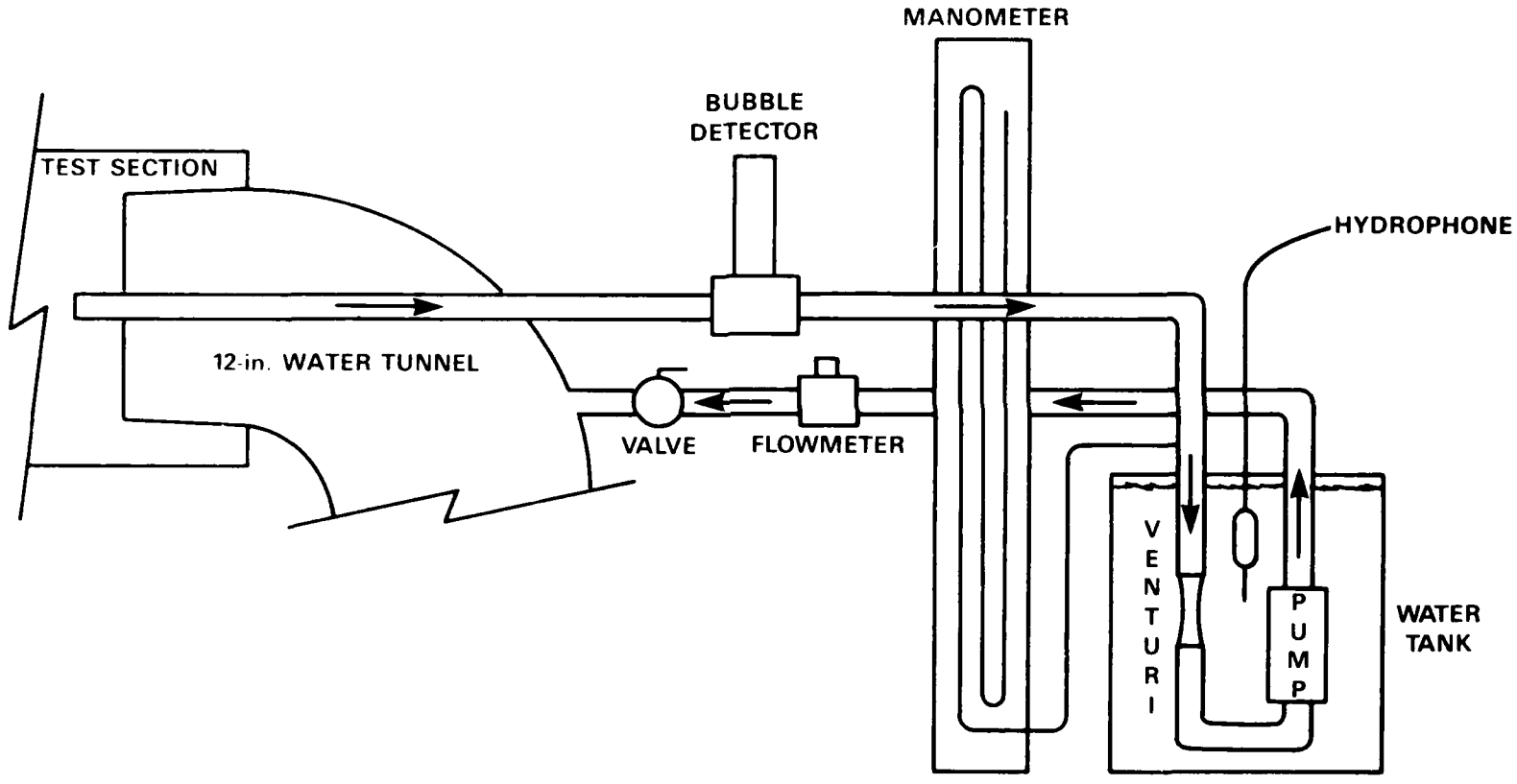


Figure 3 — Susceptibility Measurements of the 12-Inch Water Tunnel

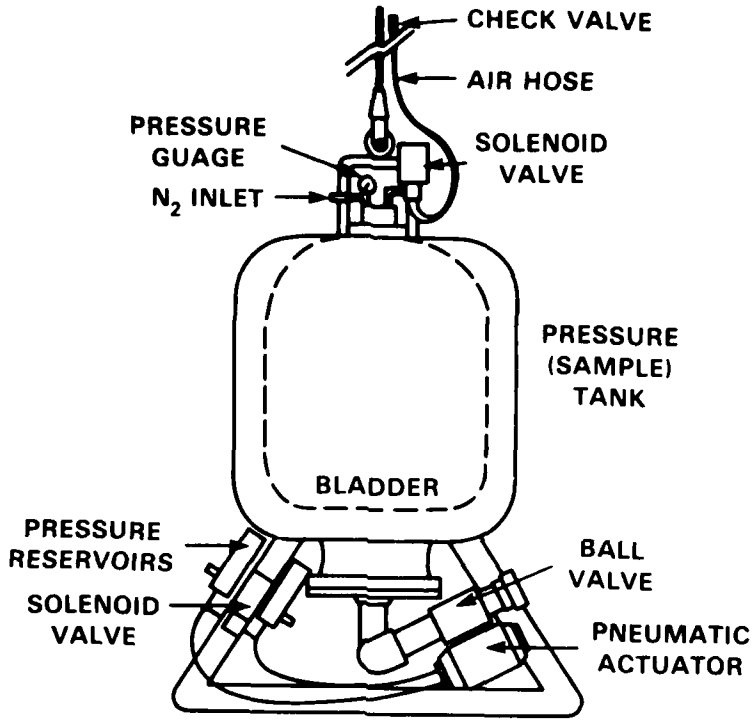


Figure 4 — Ocean Sampler

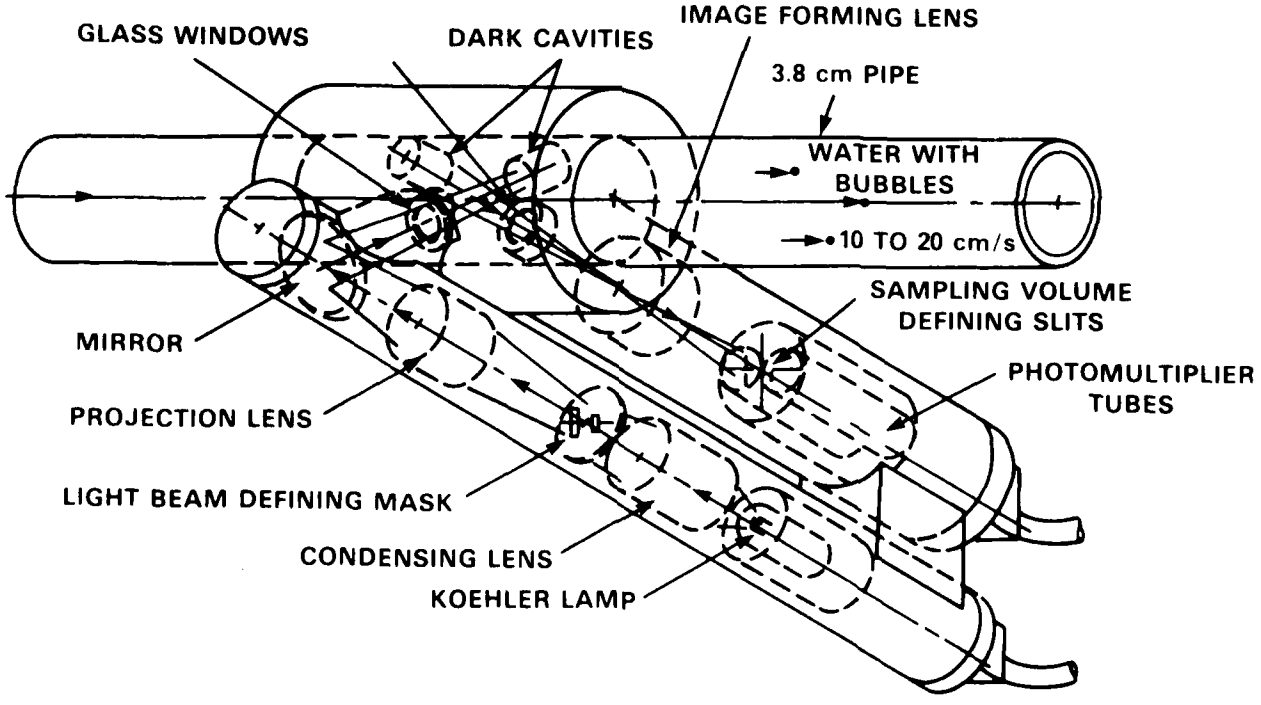


Figure 5 — Overview of Microbubble Detector

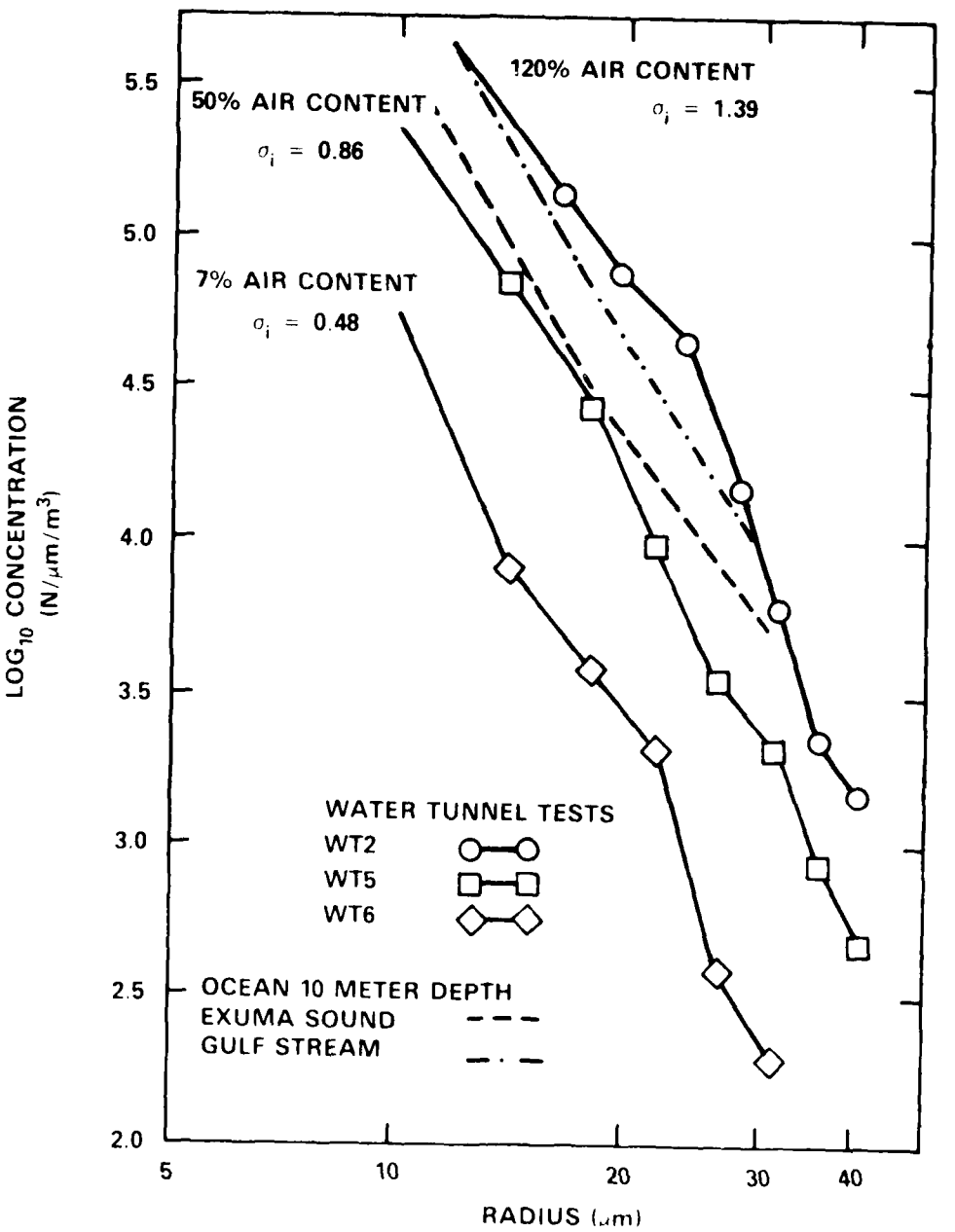


Figure 6 — Water Tunnel Microbubble Spectra, P = 1.17 bars

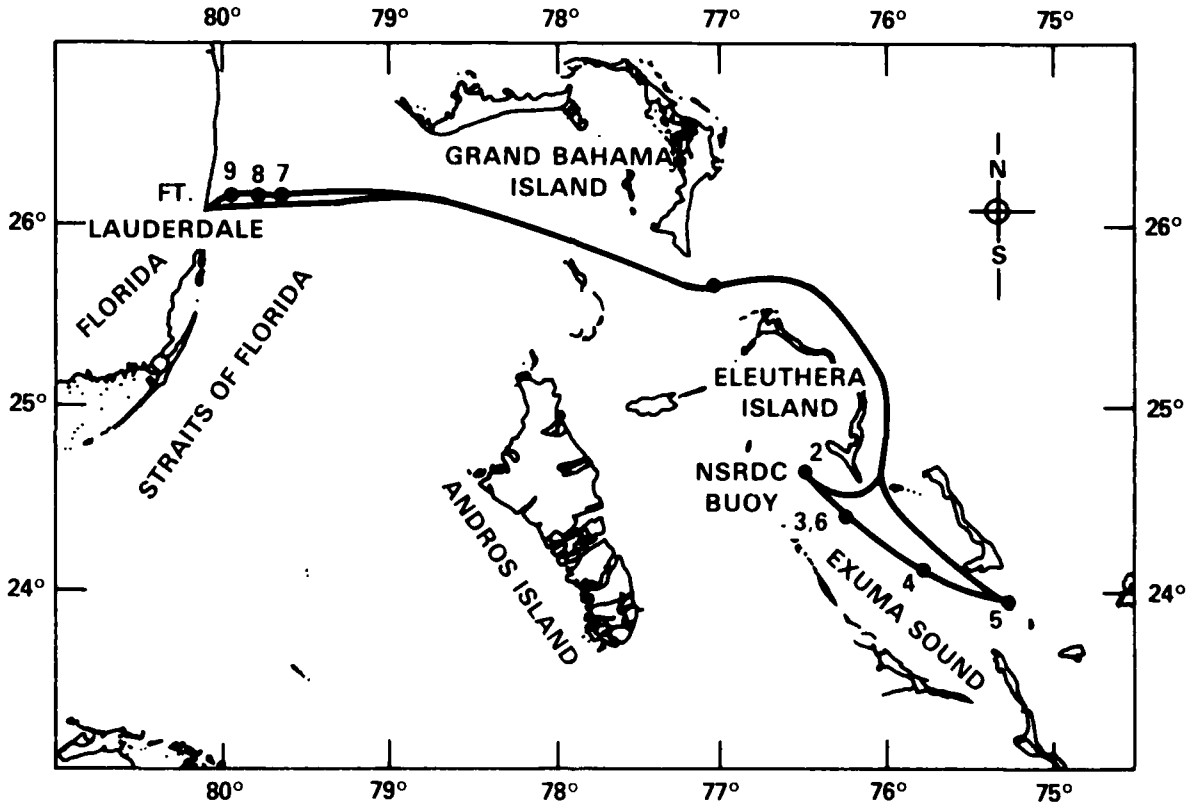


Figure 7 — Ocean Test Stations

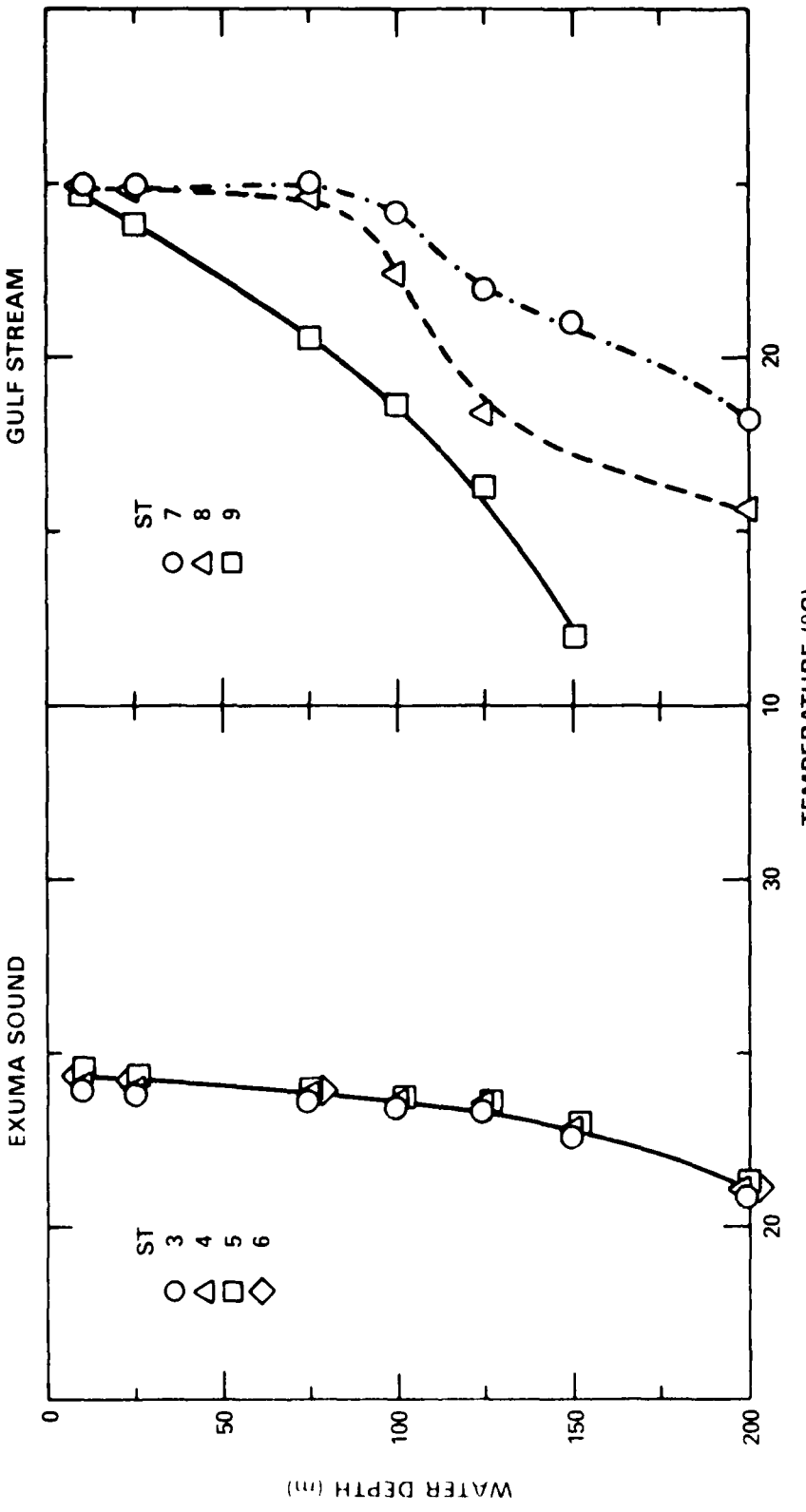


Figure 8 — Temperature Distribution in Ocean

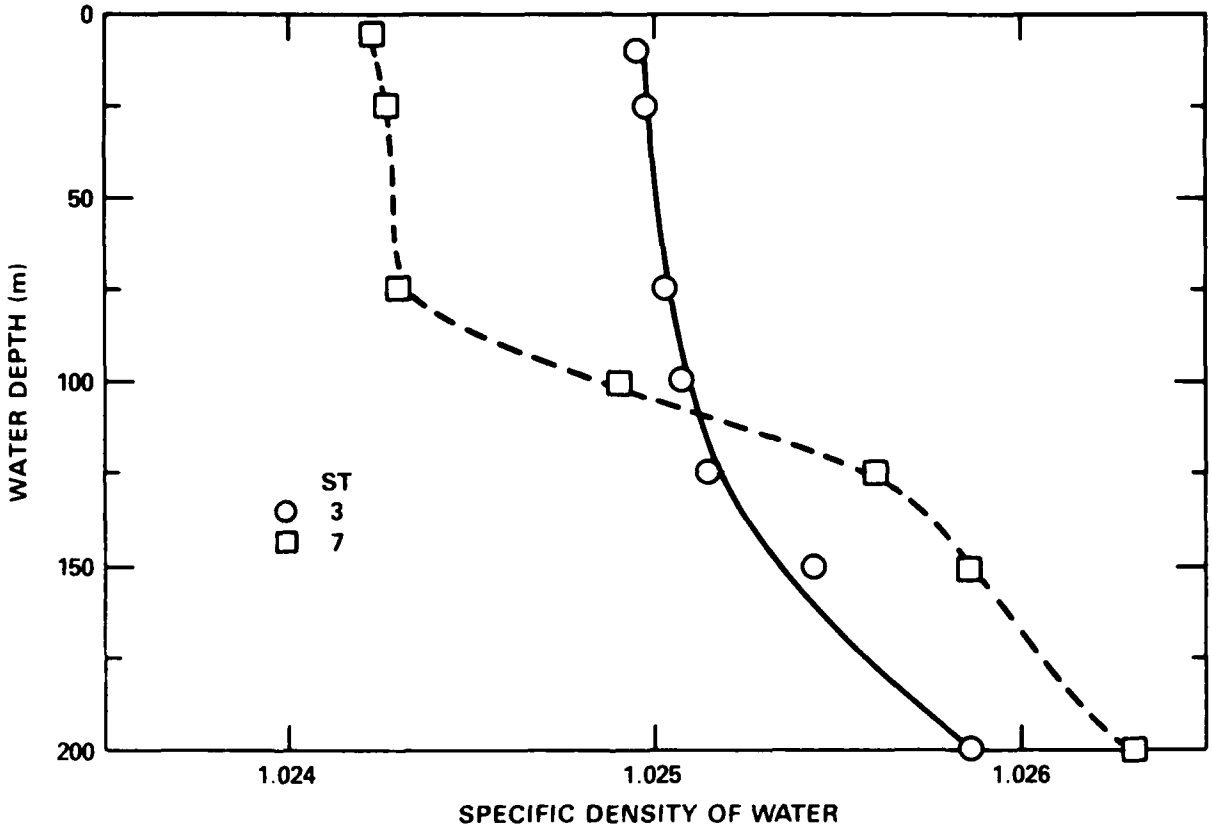


Figure 9 — Water Density Distribution in Ocean

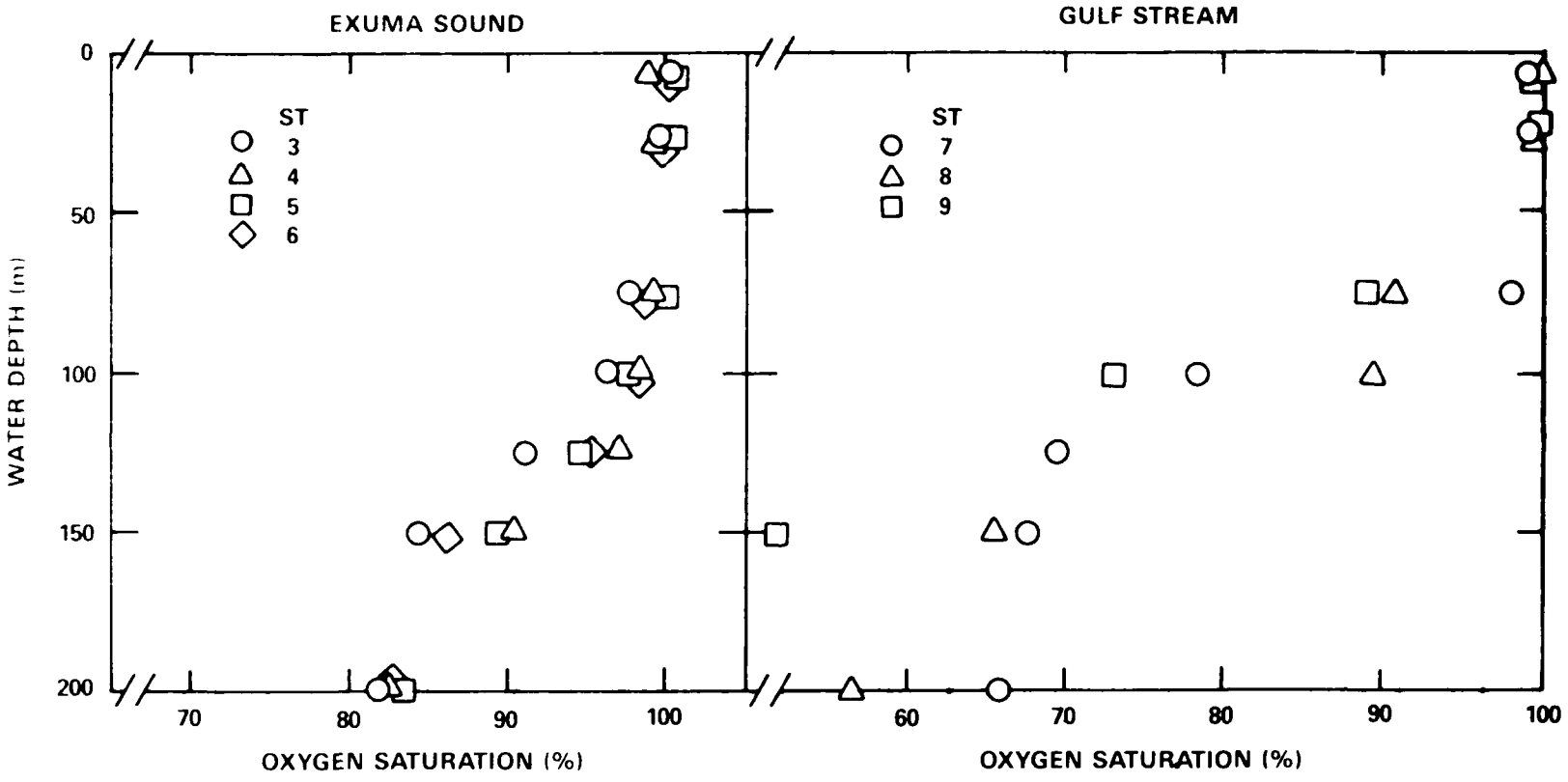


Figure 10 — Oxygen Saturation in Ocean at Standard Temperature and Atmospheric Pressure

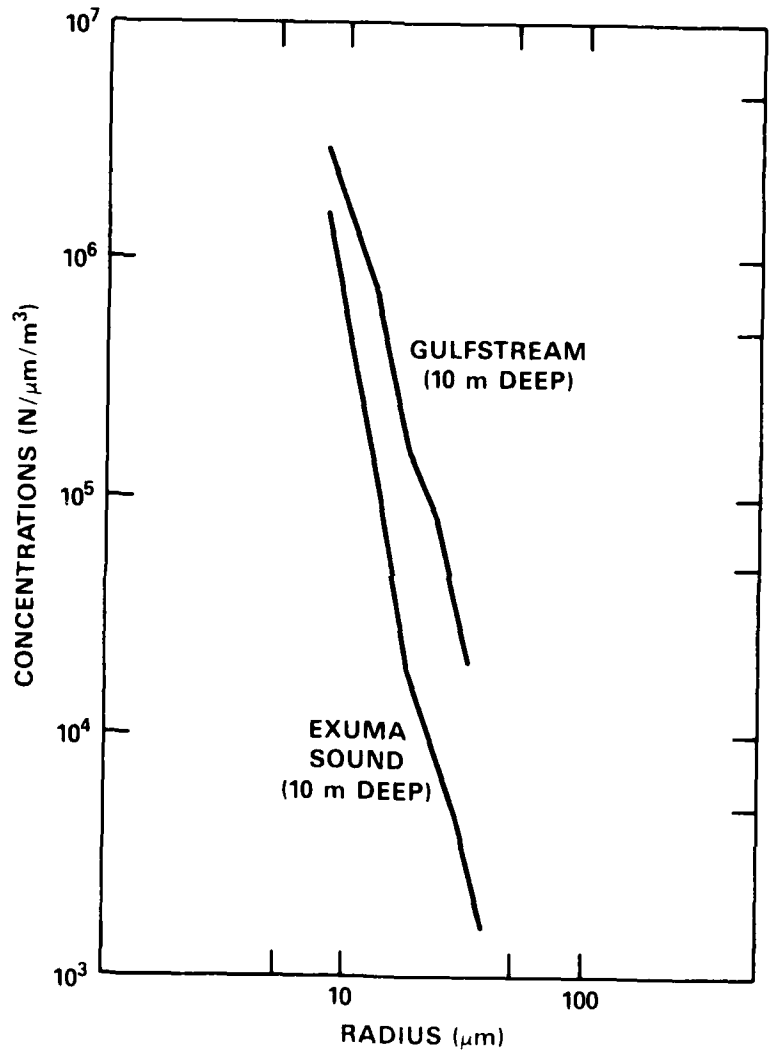


Figure 11 — Ocean Microbubbles at 10-Meter Depth

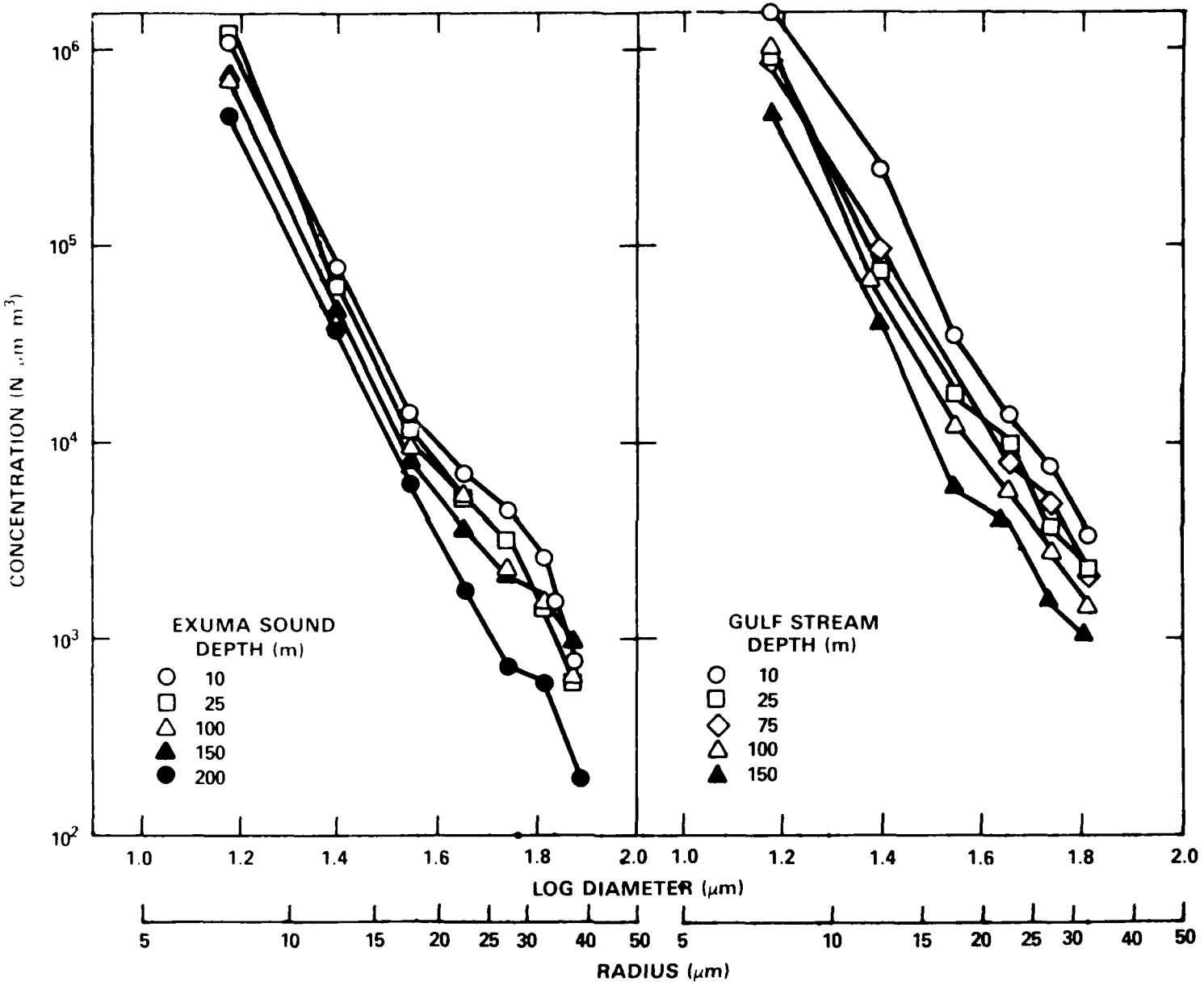


Figure 12 — Nuclei Spectra Measured in Sea Water

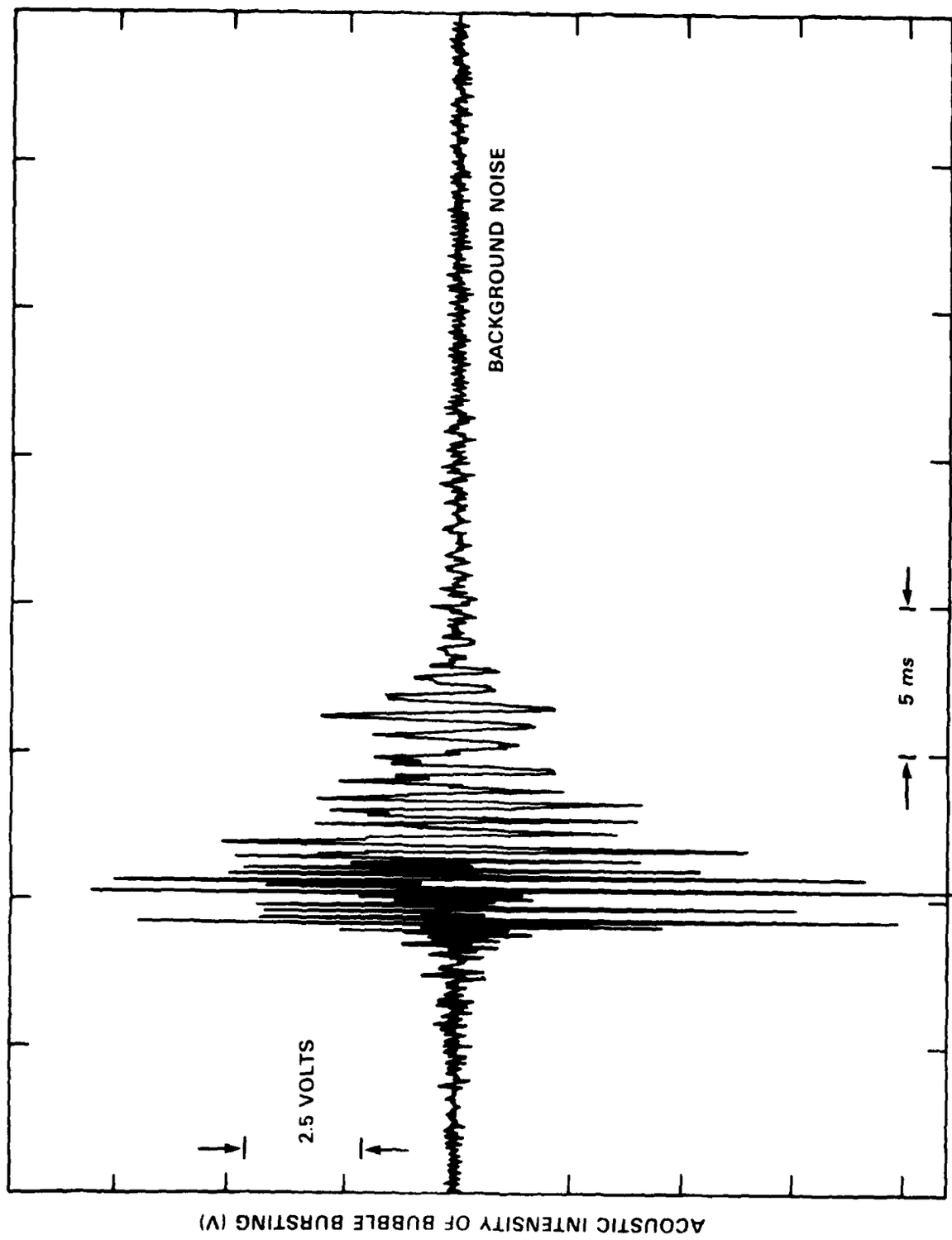


Figure 13 — A Typical Acoustic Signal from Single Bubble Bursting

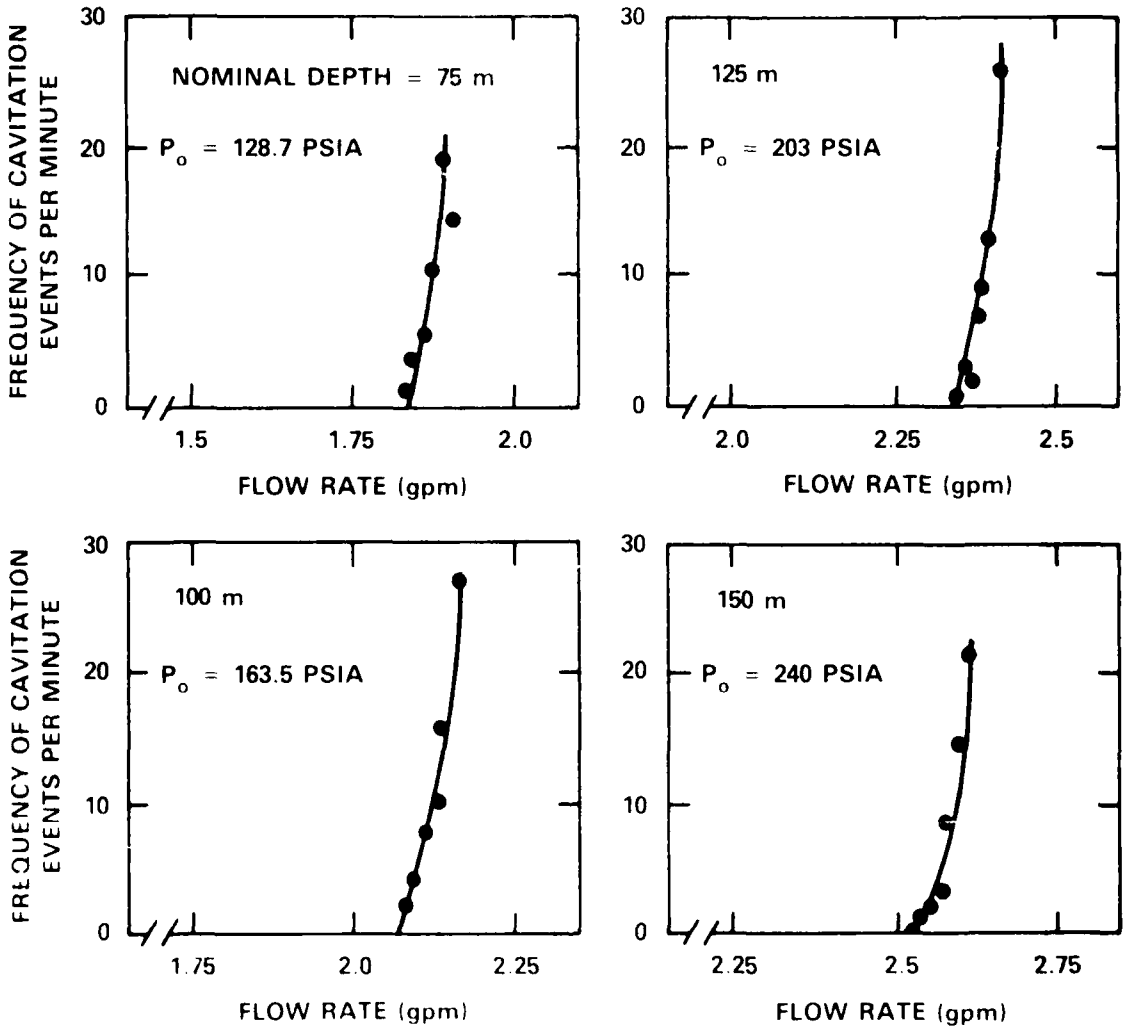


Figure 14 Cavitation Event Frequency Versus Flow Rate at Exuma Sound Station 6

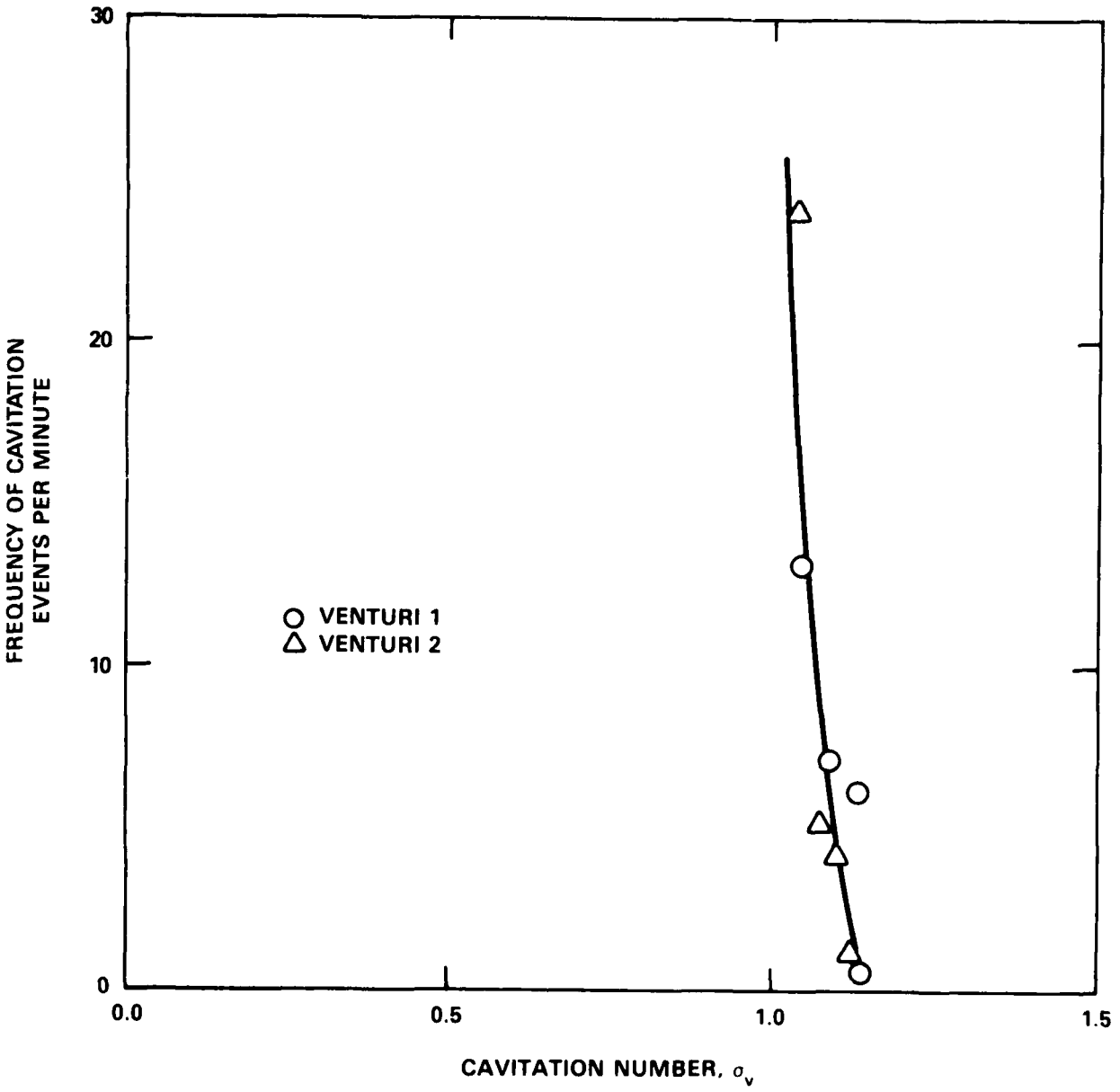


Figure 15 — Influence of Venturis on Cavitation

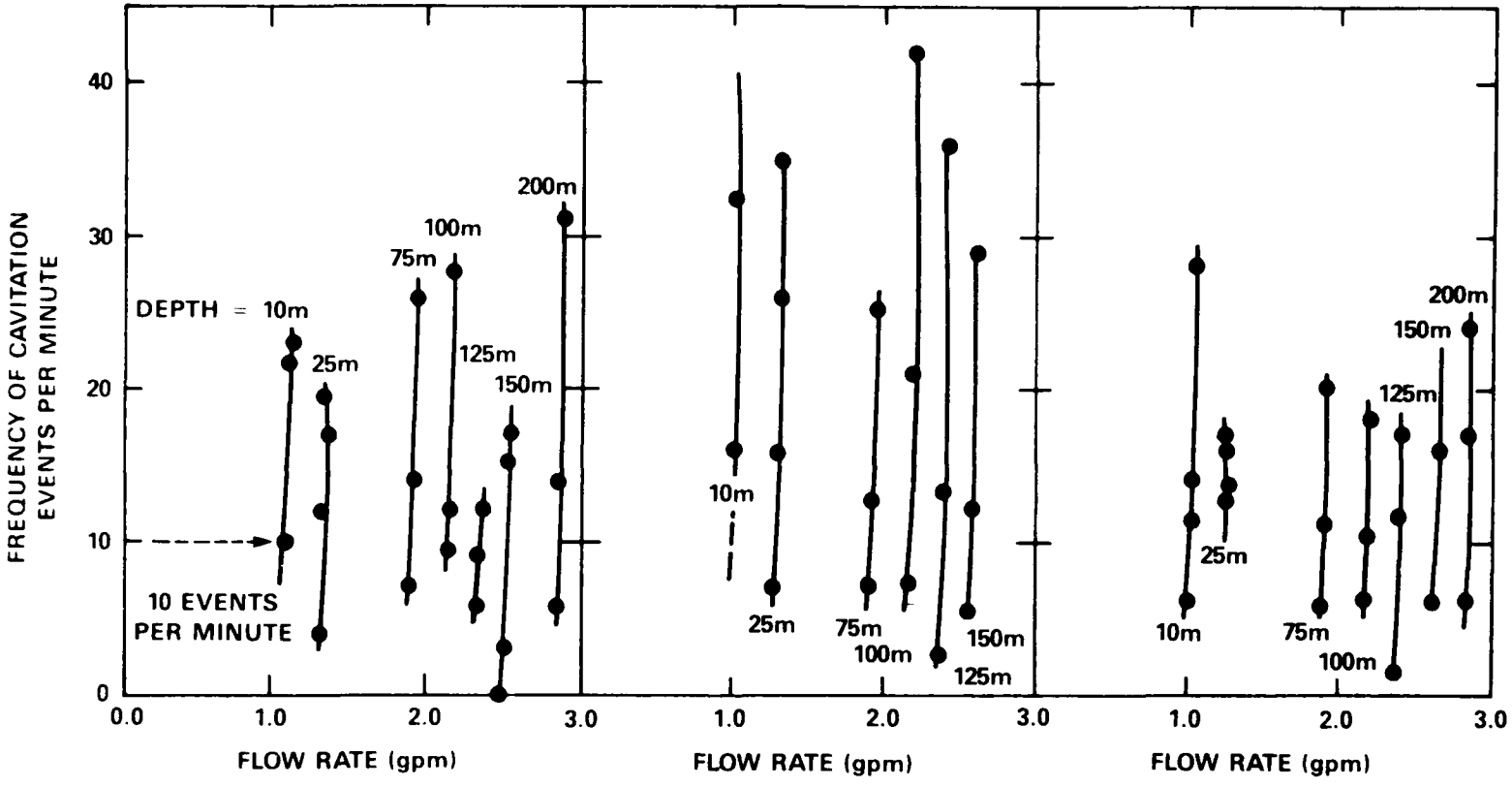


Figure 16a — Exuma Sound Station 3

Figure 16b — Exuma Sound Station 4

Figure 16c — Exuma Sound Station 5

Figure 16 — Frequency of Cavitation Events Versus Flow Rate

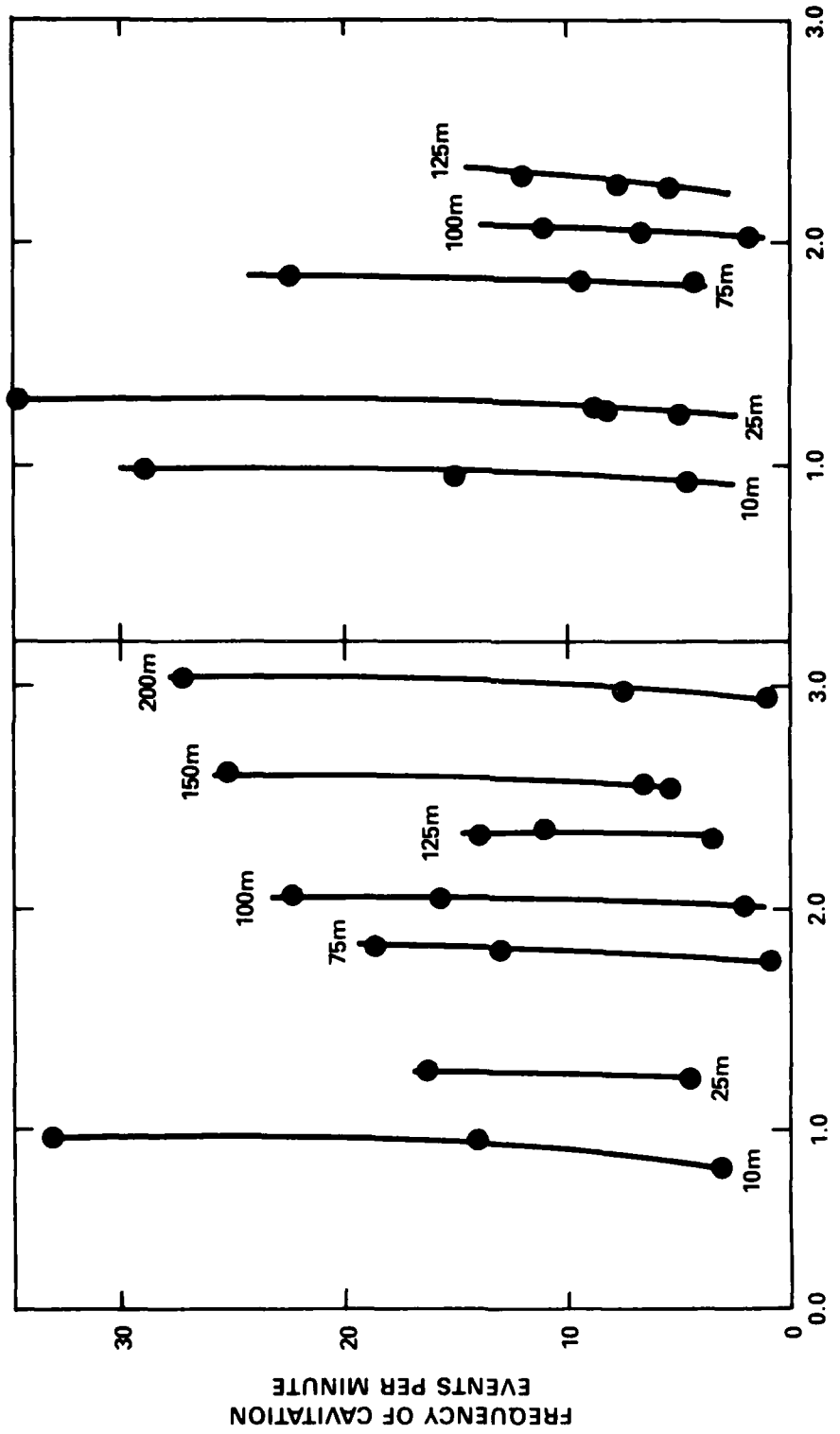


Figure 16d — Gulf Stream Station 7




Figure 16e — Gulf Stream Station 9

Figure 16 (Continued)

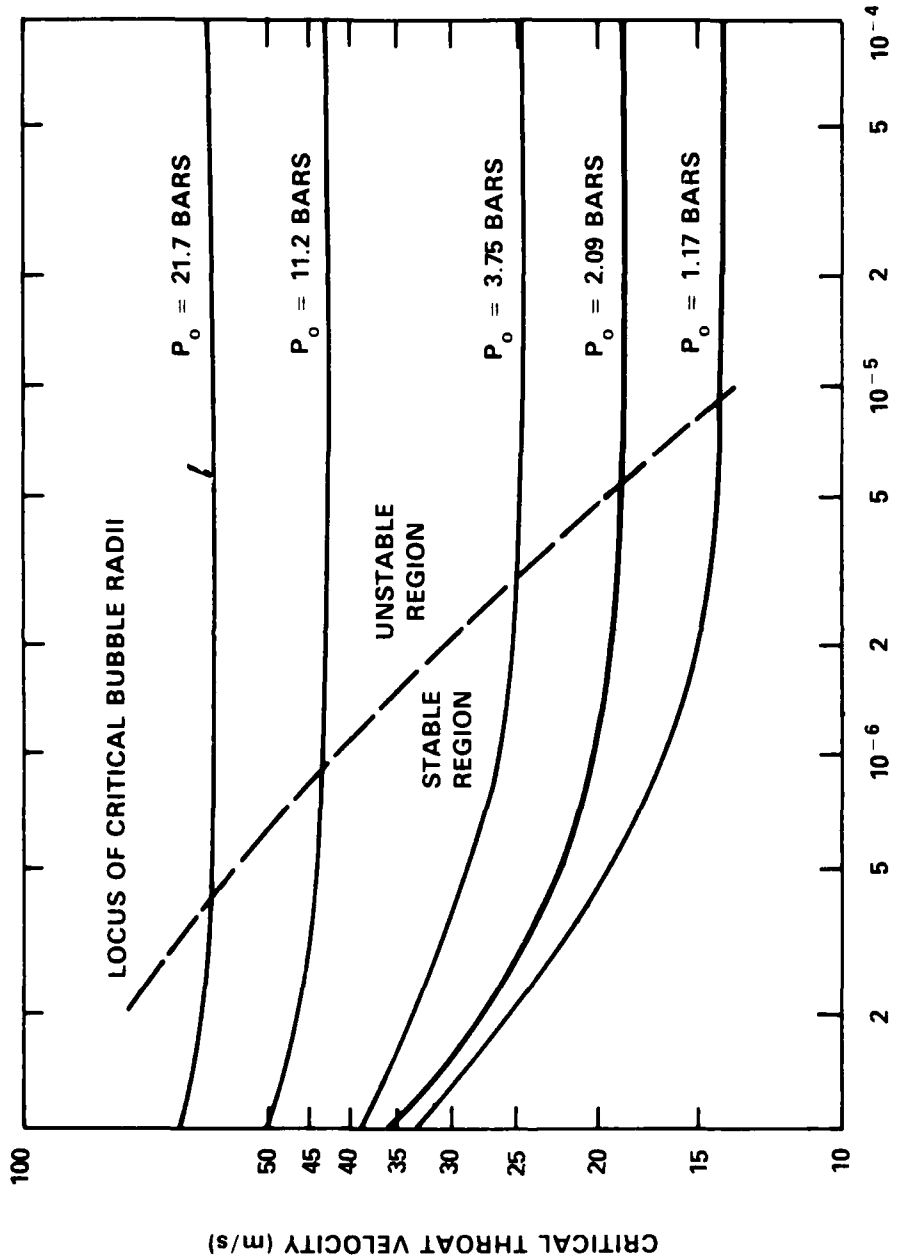


Figure 17 — Critical Bubble Radius Versus Throat Velocity

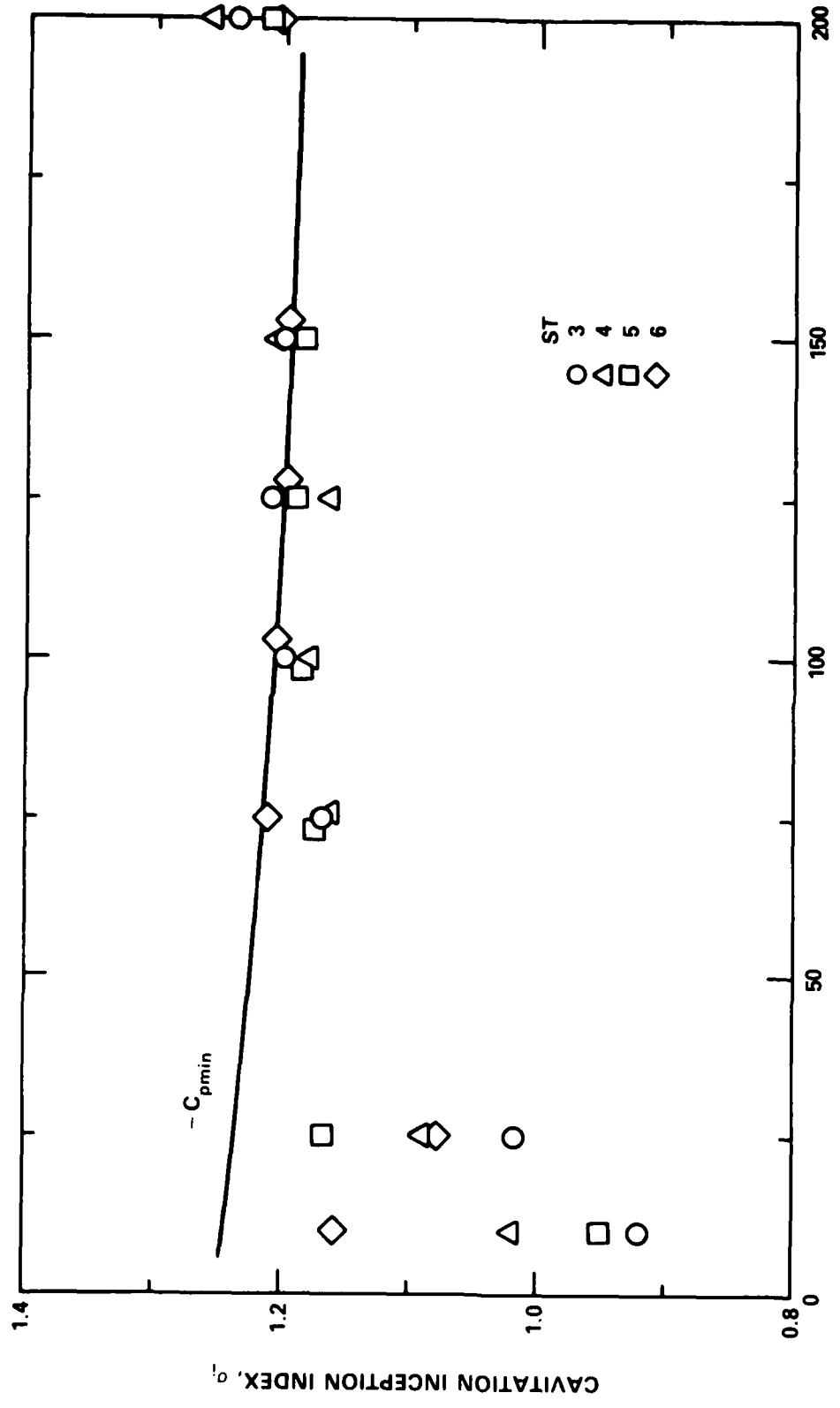


Figure 18 — Measured Cavitation Inception Index at Exuma Sound

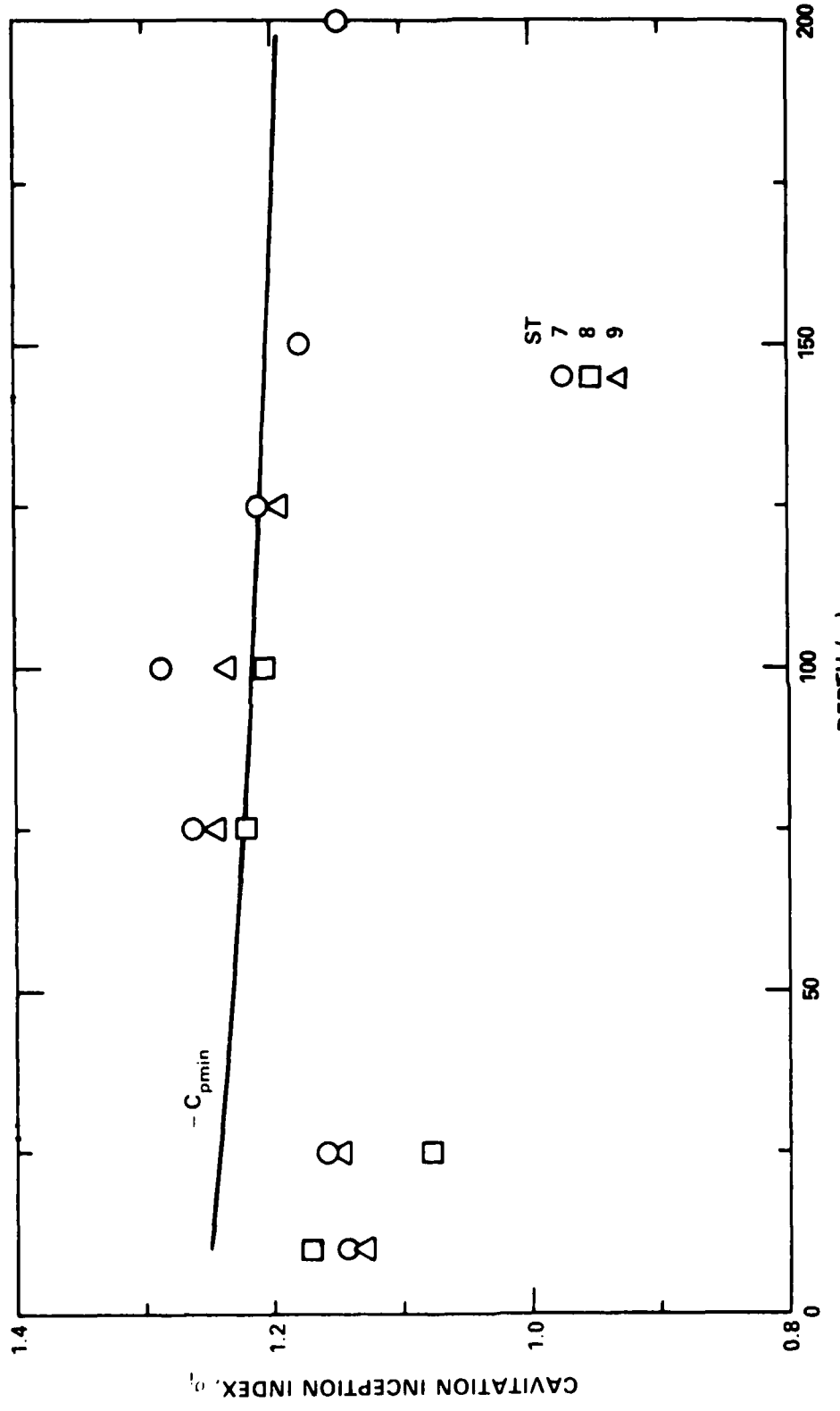


Figure 19 — Measured Cavitation Inception Index at Gulf Stream

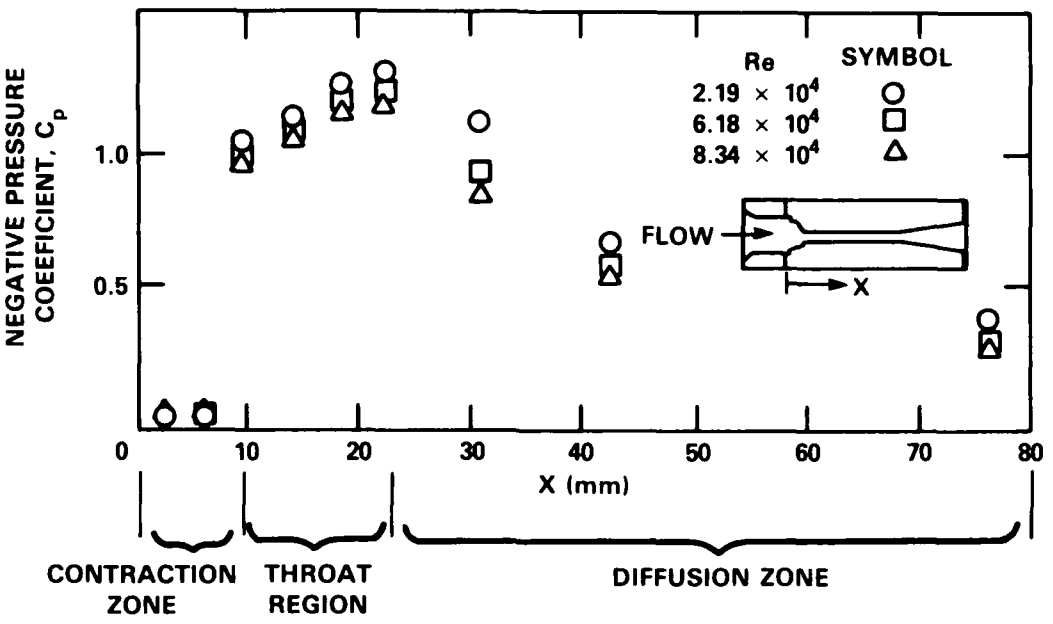


Figure 20 — *Pressure Distribution in the Venturi*

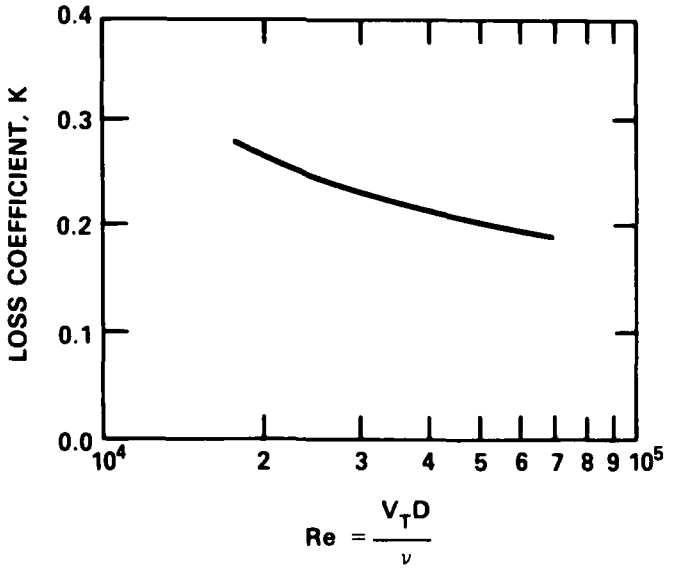


Figure 21 — Measured Loss Coefficient Versus Reynolds Number

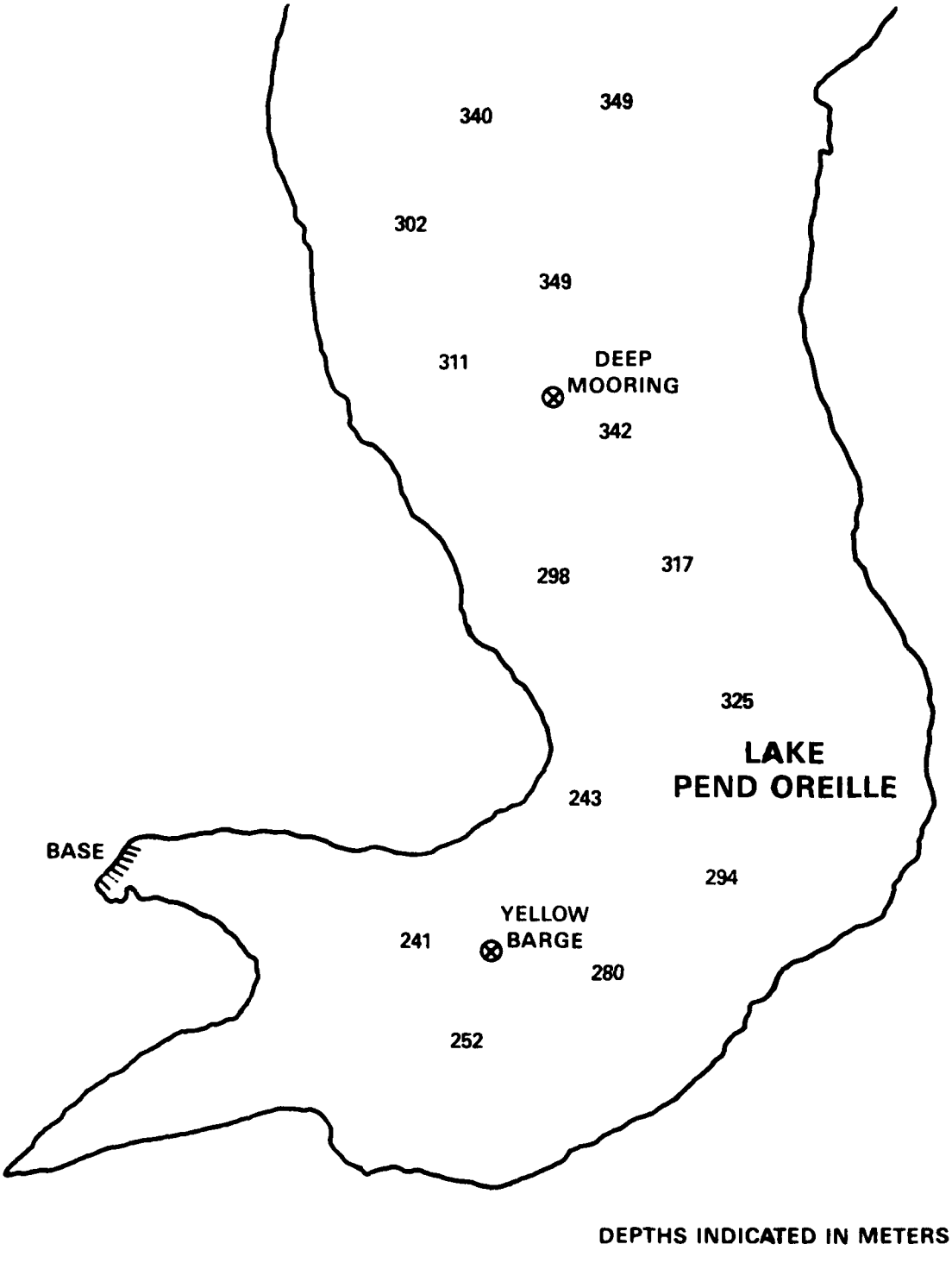


Figure 22 — Lake Pend Oreille Test Sites

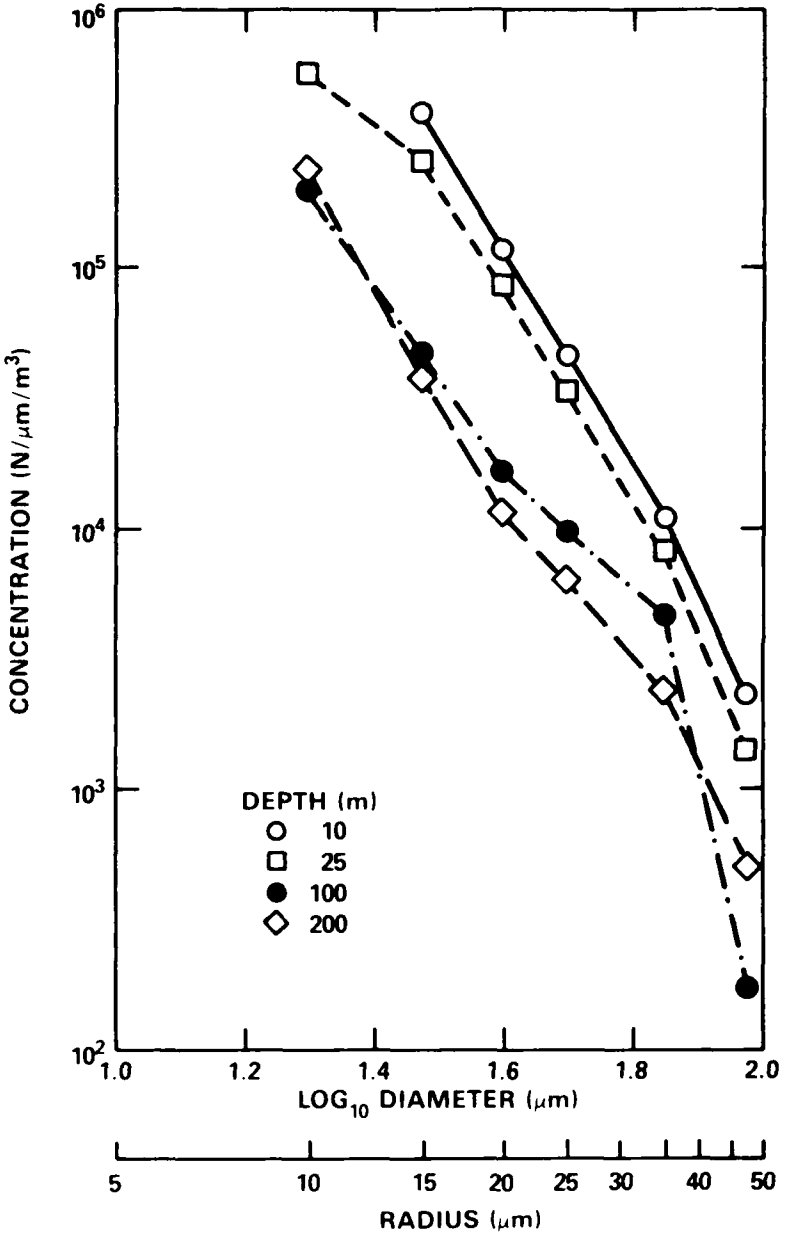


Figure 23 — Nuclei Spectra Measured at Lake Pend Oreille

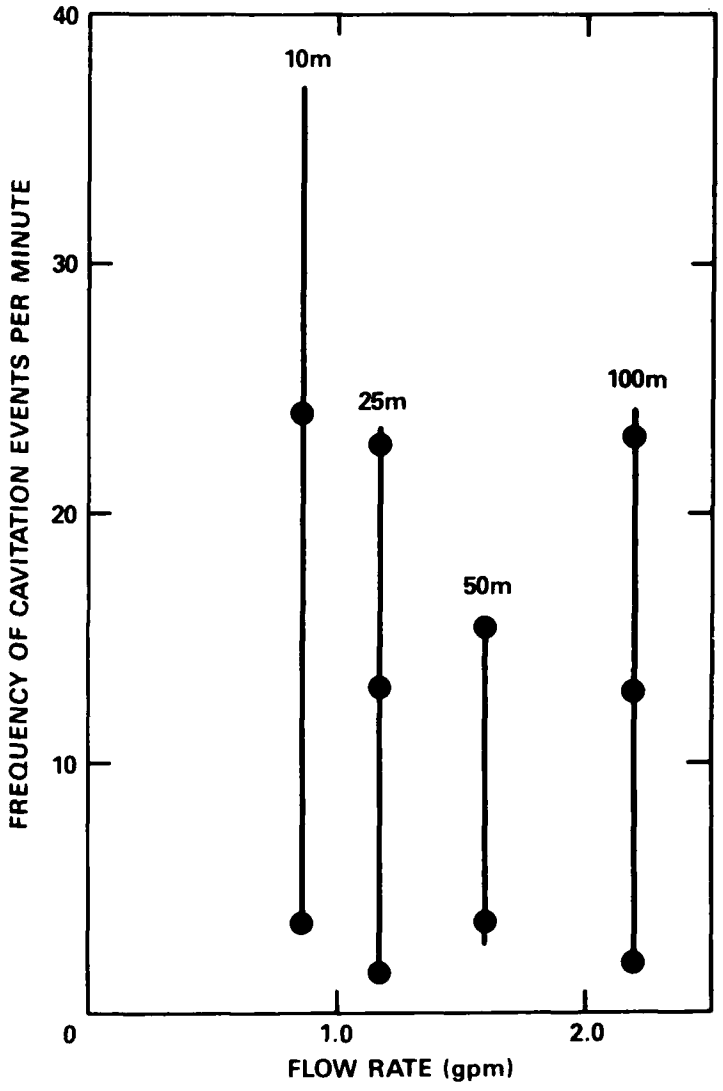


Figure 24 — Frequency of Cavitation Events Versus Flow Rate at Lake Pend Oreille

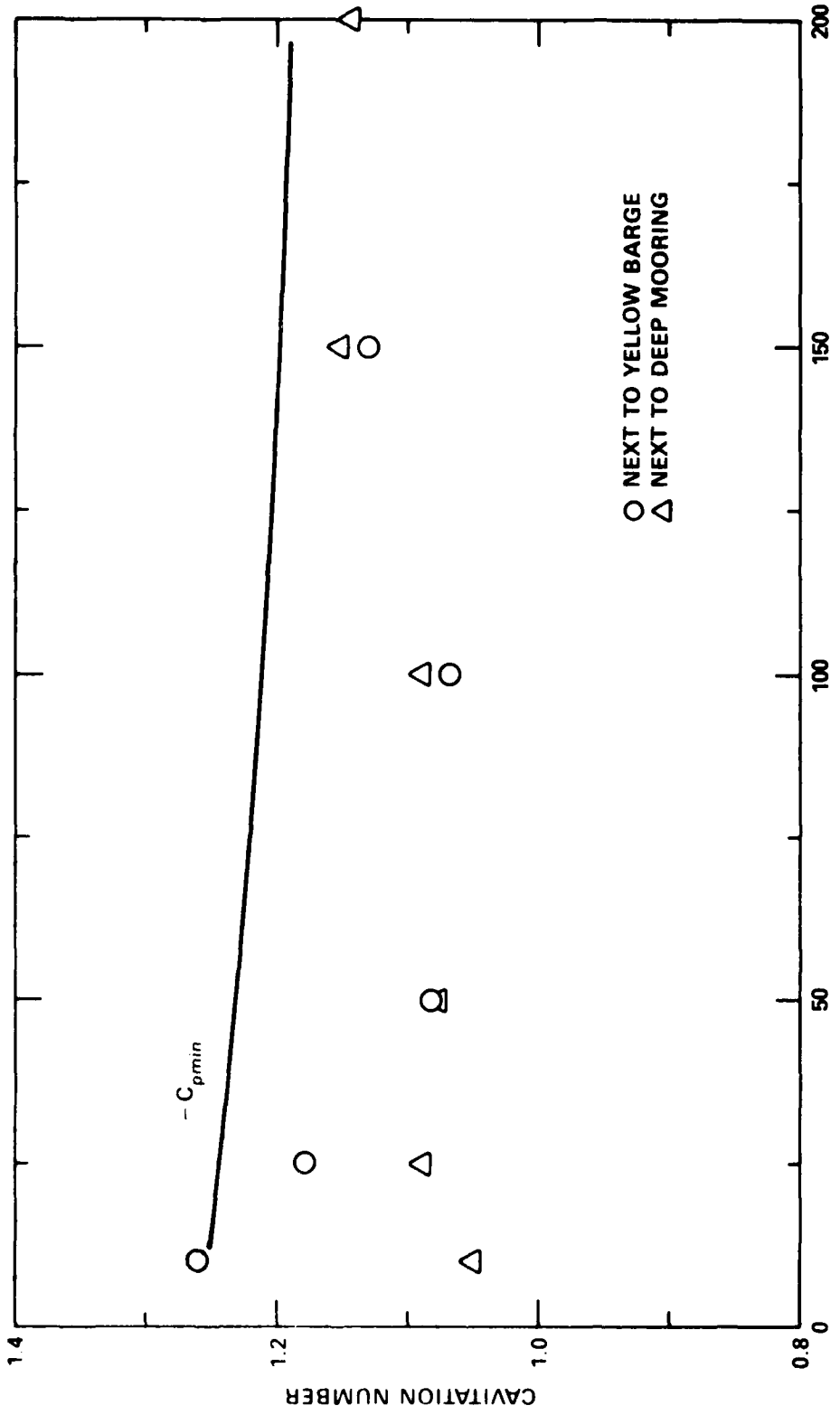


Figure 25 — Measured Cavitation Inception Index at Lake Pend Oreille

## REFERENCES


1. Acosta, A.J. and B.R. Parkin, "Cavitation Inception — A Selective Review," 17th American Towing Tank Conference Calif. Int. of Technology, Pasadena, Ca. (June 1974).

2. Kuiper, G. "Cavitation Inception on Ship Propeller Models," Ph.D. dissertation, Netherlands Ship Model Basin, Waginengen, Netherlands (March 1981).

3. Zsolnay, A., D.M. Lavoie, D.A. Wiesenburg, and D. Reid, "Environmental Parameters in Exuma Sound and the Straits of Floridas," Naval Ocean Research and Development Activity, Technical Note 252 (1984).

4. O'Hern, T.J., J. Katz, and A.J. Acosta, "Holographic Measurements of Cavitation Nuclei in the Sea," Cavitation and Multiphase Flow Forum, American Society of Mechanical Engineers, Albuquerque, N.M. (1985).

5. Brockett, T., "Computational Method for Determination of Bubble Distributions in Liquids," DTNSRDC Report No. 2798 (April 1969).

6. Ripkin, J.R. and A.P. Killen, "Gas Bubbles: Their Occurrence, Measurement, and Influence in Cavitation Testing," Proceedings IAHY Symposium, Sendai, Japan (1962).

7. LeGoff, J.P. and Y. Lecoffre, "Nuclei and Cavitation," 14th Symposium on Naval Hydrodynamics, Ann Arbor, Mich. (1982).

8. Gowing, S. and S.C. Ling, "Measurements of Microbubbles in a Water Tunnel," 19th American Towing Tank Conference at University of Michigan, Ann Arbor, Mich. (July 1980).

9. Ling, S.C., S. Gowing, and Y.T. Shen, "The Role of Microbubbles on Cavitation on Head-forms," 14th Symposium on Naval Hydrodynamics. Ann Arbor, Mich. (1982).

10. Katz, J., S. Gowing, T. O'Hern, and A. Acosta, "A Comparative Study Between Holographic and Light Scattering Techniques of Microbubble Detection," International Union of Theoretical and Applied Mechanics Symposium—Measuring Techniques in Gas-Liquid Two-Phase Flows, Nancy, France (1983).

11. Knapp, R.T., J.W. Daily, and F.G. Hammitt, "Cavitation," McGraw-Hill, New York (1970).

12. Medwin. H., "In Situ Acoustic Measurements of Microbubble at Sea," Journal of Geophysics Research, Vol. 82 (1977).

13. Weitendorf, E.A., "Conclusions from Full-Scale and Model Investigations of the Free Air Content and of the Propeller-Excited Hull Pressure Amplitudes Due to Cavitation," International Symposium on Cavitation Inception, American Society of Mechanical Engineers, New York City (Dec 1979).

14. Medwin, H., "Acoustic Bubble Spectra at Sea," Proceedings of First International Conference on Cavitation and Inhomogeneities in Underwater Acoustics, Gottingen, Fed. Republic of Germany (1979).

15. Shen, Y.T. and F.B. Peterson, "Cavitation Inception — A Review — Progress Since 19th ATTC," 20th American Towing Tank Conference, Stevens Int. of Technology, Hoboken, N.J. (1983).

16. Godefroy, H.W., R.J. Jansen, A.P. Keller, Y. Lecoffre, D.M. Oldenziel, and R.L. van Renesse, "Comparison of Measuring and Control Methods of the Water Quality with Respect to Cavitation Behavior," Delft Hydraulic Laboratory, Delft, Netherlands (1981).

17. Shen, Y.T., S. Gowing, and R. Pierce, "Cavitation Susceptibility Measurements by a Venturi," International Symposium on Cavitation Inception, Winter Annual Meeting of American Society of Mechanical Engineers, New Orleans, La. (Dec 1984).

18. d'Agostino, L. and A.J. Acosta, "On the Design of Cavitation Susceptibility Meters," 20th American Towing Tank Conference, Stevens Int. of Technology, Hoboken, N.J. (1983).

19. Chahine, G. and Y.T. Shen, "Bubble Dynamics and Inception in Cavitation Susceptibility Meters," Winter Annual Meeting of American Society of Mechanical Engineers, Miami, Fla. (1985).

20. Shen, Y.T. and S. Gowing, "Scale Effect on Bubble Growth and Cavitation Inception in Cavitation Susceptibility Meters," Cavitation and Multiphase Flow Forum, American Society of Mechanical Engineers, Albuquerque, NM (1985).

21. Schlichting, H., "Boundary Layer Theory," McGraw-Hill, New York (1979).

22. Crump, S., "Determination of Critical Pressures for the Inception of Cavitation in Fresh and Sea Water as Influenced by Air Content of the Water," DTMB Report 575 (1949).

23. Crump, S., "Critical Pressures for the Inception of Cavitation in a Large-Scale Numachi Nozzle as Influenced by the Air Content of the Water," DTMP Report 770 (1951).

24. Ligneul, P., "Influence of Nuclei on Cavitation of Marine Propellers," Association Technique Maritime et Aeronautique, Paris, France (1984).

## INITIAL DISTRIBUTION

| Copies | |
|---|---|
| 1 | NOP 21T3 (A. Bisson) |
| 5 | NAVSEA<br>1 05R<br>2 55N<br>1 55W33<br>1 56X12 |
| 1 | CONR 23 |
| 1 | CONR 432/Arlington (C. Lee) |
| 1 | ONR 425 (D.L. Bradley) |
| 1 | NORDA/Mississippi (A. Zsolnay) |
| 10 | NORDA/Mississippi (B. Eckstein) |
| 1 | NOSR 2501 (J. Hoyt) |
| 1 | U.S. Naval Academy (R. Johnson) |
| 12 | DTIC |
| 1 | CIT (A. Acosta) |
| 1 | MIT (J. Kerwin) |
| 1 | Univ of Iowa (F. Stones) |
| 1 | Univ of Michigan (W. Vorus) |
| 1 | Univ of Minnesota (R. Arndt) |
| 1 | Penn State Univ (B. Parkin) |
| 1 | Penn State Univ (W. Holl) |
| 1 | Penn State Univ (M. Billet) |
| 1 | Purdue Univ (J. Katz) |
| 1 | Traco Hydronautics (G. Chahine) |

CENTER DISTRIBUTION

| Copies | Code | Name |
|---|---|---|
| 1 | 012.3 | Moran |
| 1 | 15 | Morgan |
| 1 | 1504 | Monacella |
| 1 | 152 | Lin |
| 3 | 1522 | Remmers, Lawler, Hsu |
| 1 | 154 | McCarthy |
| 1 | 1540.2 | Cumming |
| 1 | 1541 | Rispin |
| 1 | 1542 | Huang |
| 20 | 1542 | Shen |
| 15 | 1542 | Gowing |
| 1 | 1543 | Rood |
| 1 | 1544 | Peterson |
| 1 | 1544 | Jessup |
| 1 | 156 | Cieslowski |
| 1 | 19 | Sevik |
| 1 | 19 | Strasberg |
| 1 | 1905 | Blake |
| 1 | 192 | Smith |
| 1 | 194 | Archibald |
| 1 | 1944 | Maga |
| 1 | 1946 | Spina |
| 10 | 5211.1 | Reports Distribution |
| 1 | 522.1 | TIC (C) |
| 1 | 522.2 | TIC (A) |

END

DTIC

7-86